A Dissertation for the Degree of Doctor of Philosophy

Beneficial effects of gingerenone A, a polyphenol present in ginger, on obesity and metabolic disorders

생강의 폴리페놀 성분인 진저레논 에이의
비만과 대사성 질환 개선 효능

By
Sujin Suk

Interdisciplinary Program in Agricultural Biotechnology
Seoul National University

August, 2015

Beneficial effects of gingerenone A, a polyphenol present in ginger, on obesity and metabolic disorders

By

Sujin Suk

Dissertation
Submitted as partial fulfillment of the requirements
for the degree of Doctor of Philosophy

under the supervision of Professor Ki Won Lee

at the
Seoul National University

August, 2015

Beneficial effects of gingerenone A, a polyphenol present in ginger, on obesity and metabolic disorders

생강의 폴리페놀 성분인 진저레논 에이의
비만과 대사성 질환 개선 효능

지도교수 이 기 원

이 논문을 박사학위 논문으로 제출함
2015 년 8 월
서울대학교 대학원
협동과정 농업생물공학전공
석 수 진
석수진의 박사 학위논문을 인준함
2015 년 8 월

위 원 장 : 하 남 출 (인)

부위원장 : 이 기 원 (인)

위 원 : 서 정 용 (인)

위 원 : 윤 정 한 (인)

위 원 : 이 홍 진 (인)

Abstract

The World Health Organization (WHO), defines both overweight and obesity as potentially hazardous conditions of abnormal or excessive fat accumulation arising from an imbalance between energy intake and energy expenditure. Several studies have shown that excessive bodily adipose tissue is associated with metabolic disorders including type 2 diabetes, cardiovascular disease, and non-alcoholic fatty liver disease. Therefore, the inhibition of adipose tissue expansion has been proposed as a promising strategy for the prevention and/or treatment of obesity.

Ginger is frequently used as an ingredient in nonprescription weight-loss products. Although several pharmacological effects of ginger extract on obesity and metabolic disease have been studied, the relative potencies of the major bioactive ginger compounds (6-gingerol (6G), 8-gingerol (8G), 10-gingerol (10G), 6-shogaol (6S) and gingerenone A (GA)) for the suppression of adipogenesis and lipid accumulation have not been clearly elucidated.

In the present study, I first compared the effect of the gingerols, 6S and GA on adipogenesis in 3T3-L1 preadipocytes.

Our findings show that GA elicits the most potent inhibitory effect on adipogenesis in 3T3-L1 preadipocytes among the five ginger compounds. GA consistently inhibited the expression of adipogenesis- and lipogenesis-related proteins in a concentration-dependent manner. I next compared the effect of the compounds on lipid accumulation in fully differentiated 3T3-L1 adipocytes. The results revealed that only GA reduces lipid accumulation in mature adipocytes, by regulating fatty acid metabolism, showing that GA inhibits not only adipogenesis in preadipocytes but also lipid accumulation in mature adipocytes.

On the basis of these results, I further investigated the effect of GA on body weight gain induced by a high-fat diet (HFD). Consistent with the *in vitro* data, GA supplementation significantly attenuated HFD-induced obesity by reducing fat mass. Significant losses of fat mass can cause lipodystrophy, leading to ectopic lipid deposition, particularly in the liver. Thus, I chose to investigate serum and liver lipid profiles to examine the effect of GA on lipodystrophy. Circulating free fatty acids (FFAs) and hepatic triacylglycerol (TAG) content were ameliorated to some extent by

treatment with GA when comparisons were made to the HFD-alone group. These results suggest that GA suppresses HFD-induced obesity by reducing adipose tissue mass, but does not affect lipodystrophy. To further investigate the mechanisms involved in the reduction of GA-induced fat mass, I evaluated fatty acid metabolism in epididymal adipose tissue (EWAT). The results showed that GA reduces the expression of lipolysis- and lipogenesis-related proteins, while increasing fatty acid oxidation- and mitochondrial biogenesis-related transcript levels via the activation of AMP-activated protein kinase (AMPK) in EWAT.

Adipose tissue inflammation caused by excessively hypertrophied fat mass has been closely associated with insulin resistance. I investigated whether the anti-obesity effect of GA might be influencing adipose tissue inflammation and glucose metabolism, and found that GA effectively suppressed adipose tissue inflammation by blocking macrophage recruitment and down-regulating expression of the pro-inflammatory cytokine, tumor necrosis factor α (TNF-α). Moreover, GA increased the expression levels of adiponectin, an adipokine with anti-

inflammatory and insulin-sensitizing properties. Next, I examined the effect of GA on insulin resistance by conducting a hyperinsulinemic-euglycemic clamp experiment, as such effects on adipose tissue inflammation and adiponectin expression may also affect glucose metabolism. GA effectively improved glucose intolerance induced by high-fat feeding via an increase in whole-body glucose utilization.

In conclusion, I observed that GA suppressed the development of obesity and adipose tissue inflammation, while improving glucose intolerance induced by HFD in mice, highlighting GA's potential for development as a therapeutic agent for the treatment of obesity and its complications.

Keywords : Gingerenone A, obesity, adipose tissue inflammation, glucose intolerance, fatty acid metabolism

Student ID : 2011-30346

Contents

Chapter 1.

Beneficial effects of ginger (*Zingiber officinale* Roscoe), on obesity and its complications: A Review

Abstract

Ginger, *Zingiber officinale (Z. officinale)* Roscoe, has historically been used as a spice and herbal medicine ingredient in Korea, China, and India. Recent studies have investigated ginger extract for the prevention and/or treatment of obesity, insulin resistance, type 2 diabetes, and non-alcoholic fatty liver disease. Ginger is largely composed of volatile oils, non-volatile pungent components, and diarylheptanoid compounds. In this review, I summarize the effects of ginger and its components on obesity and its complications. In addition, the article discusses the anti-obesity and anti-metabolic disease therapeutic potential of ginger and analyzes the molecular mechanisms of action responsible.

1.1. Introduction

The rising incidence of obesity has been characterized as an epidemic of global proportions, and its prevalence has increased dramatically over the last several decades [1, 2]. Obesity is characterized by the accumulation of excessive fat and is caused by an imbalance between energy intake and energy expenditure [3]. Several studies have shown that excessive adipose tissue is associated with metabolic disorders including type 2 diabetes, cardiovascular disease, and non-alcoholic fatty liver disease [4-6]. Chronic low-grade inflammation has also been identified as a link between obesity and insulin resistance (IR) [7]. IR is a condition involving either normal or increased levels of insulin production, but in which insulin is not sufficiently effective in metabolically important tissues such as the skeletal muscle, liver and adipose tissue [1]. The condition is a major risk factor for, and symptom of, a number of metabolic diseases, including type 2 diabetes.

Historically, ginger has had a reputation for efficacy in alleviating symptoms such as vomiting, sea sickness, cough, and indigestion [8, 9]. As well as fibrous material, ginger is composed

of volatile oils (e.g. zingeberene, farnesene), non-volatile pungent components (e.g. gingerol, shogaol), and diarylheptanoid compounds [10]. Recent studies have demonstrated that ginger and its compounds possess numerous bioactive properties including antioxidant, anti-inflammatory, and anti-cancer effects [11]. Here, I review the effects and molecular mechanisms of action responsible for the effects of ginger extract on obesity and its complications, an area that has received relatively little attention.

1.2. Beneficial effect of ginger and its constituents on obesity

1.2.1. Ginger and its constituents inhibit adipogenesis

An enlarged fat mass characteristic of obesity can result from both increases in adipocyte cell number (hyperplasia) and cell size (hypertrophy) [12]. Adipogenesis is the process by which the preadipocytes differentiate into lipid-laden adipocytes, via the hyperplasia and hypertrophy [13]. Thus, the inhibition of these processes behind adipogenesis has been suggested as a promising

therapeutic approach for the prevention and treatment of obesity.

An *in vitro* adipogenesis study of 6-gingerol was conducted using 3T3-L1 preadipocytes. The effect of 6-gingerol on adipogenesis was found to correlate with attenuation of the Akt/GSK3β pathway, and downregulated PPARγ and C/EBPα expression [14]. The effect of 6-gingerol has been reconfirmed in a further study using a rosiglitazone-induced 3T3-L1 adipogenesis model [15].

1.2.2. Ginger and its constituents inhibit amylase and pancreatic lipase activity

Amylase and lipase are two enzymes that catalyze the hydrolysis of carbohydrates and lipids, respectively. In obese states, hydrolysis of dietary starch and fat can accelerate adipocyte hypertrophy as well as hyperlipidemia [16, 17]. For this reason, amylase and pancreatic lipase inhibitors are considered to be valuable therapeutic reagents for the treatment of diet-induced obesity [17]. Orlistat, a pancreatic lipase inhibitor, has long been used as an anti-obesity medication [18].

An *in vivo* study revealed that oral supplementation with 6-gingerol (75 mg/kg/day) reduced body weight gain in rats fed on a high-fat diet (HFD) through the inhibition of intestinal absorption of dietary fat and the expression of α-amylase and pancreatic lipase [16].

1.2.3. Ginger and its constituents enhance fatty acid metabolism

Hypertrophied adipose tissue in obese individuals plays a role in maintaining excess levels of free fatty acids (FFAs) in the circulation. A number of studies have suggested that FFAs induce insulin resistance by inhibiting glucose uptake [19-21]. It therefore seems that the regulation of fatty acid metabolism is critical for the prevention and treatment of obesity-related complications.

It was reported that 300 mg/kg/day oral administration of an ethanol extract of *Zingiber zeumbet* (L.) Smith (EEZZ), known as the pinecone or shampoo ginger, reduced the accumulation of visceral fat in HFD-fed mice. This inhibitory effect of EEZZ on visceral fat mass resulted from enhanced fatty acid oxidation, and is likely mediated by the up-regulation of hepatic PPARα [22].

1.3. Beneficial effects of ginger and its constituents on metabolic disorders

1.3.1. Ginger and its constituents improve hyperglycemia

In the IR state, insulin-stimulated glucose disposal is decreased, which causes hyperglycemia (high blood sugar). Chronic hyperglycemia in patients with diabetes is known to cause severe health problems such as cardiovascular disease, neuropathy, nephrophathy, and retinopathy [23].

A number of studies have examined the beneficial effects of ginger on hyperglycemia *in vitro*, *in vivo*, and in clinical trials. Li *et al*. (2012) covered the findings of these studies in a detailed review on the effect of ginger on hyperglycemia [24]. It has been recently determined that oral gavage of ethyl acetate extracts of ginger (200 mg/kg/day) for 10 weeks improves glucose intolerance in SD rats fed on a high-fat, high-carbohydrate (HFHC) diet [25]. Through *ex vivo* and *in vitro* mechanistic studies, it was found that ginger extract and its major component, 6-gingerol, improved glucose

metabolism by upregulating AMPK activity [25, 26]. Another *in vivo* study determined that rats fed with 10% ginger for 3 weeks exhibited significantly decreased levels of fasting blood glucose (by 29.81%) when compared with streptozotocin-induced diabetic rats [27]. In addition, recent clinical trials have determined that daily intake of ginger (1.6 g/day) for 12 weeks reduces fasting blood glucose, glycated hemoglobin (HbA1c), insulin, and homeostatic model assessment (HOMA) in patients with type 2 diabetes when compared to a placebo group [28]. Ginger can therefore be considered as a potential resource for further investigation to prevent the development of type 2 diabetes, via the effective management of hyperglycemia.

1.3.2. Ginger and its constituents improve dyslipidemia

IR is also closely associated with dyslipidemia. In obese and diabetic patients, elevated circulating lipid levels and ectopic lipid accumulation are commonly observed. In general, excessive FFAs released from hypertrophied adipose tissue are a risk factor for impaired glucose tolerance because they inhibit glucose

transport into metabolically important tissues including the liver and muscle.

A number of studies have determined that ginger has a beneficial effect on dyslipidemia in animal models and clinical trials. Li *et al*. (2012) described these effects in a detailed review article [24]. In summary, treatment with ginger extracts significantly reduced serum total cholesterol (TC) levels, low-density lipoprotein (LDL), TAG and FFAs, while increasing high-density lipoprotein (HDL)-cholesterol levels in animal and human studies [24].

Furthermore, a recent *in vivo* study revealed that oral supplementation with a methanol extract of ginger (500 mg/kg/day) reduced serum lipid profiles (TAG and LDL) and increased HDL levels when compared to alloxan-induced diabetic rats [29].

Clinical trials have been conducted to investigate the beneficial effects of ginger in patients with metabolic disorders. Recently, Mahluji *et al*. (2013) observed that an intake of powdered ginger (2g/day) for 2 months decreased insulin, HOMA, TAG and LDL levels in patients with type 2 diabetes when compared to the placebo group [30]. Arablou *et al*. (2014) also reported that ginger

consumption (1.6 g/day) for 12 weeks resulted in reduced lipid profiles (TG and TC) in patients with type 2 diabetes when compared to a placebo group [28].

1.3.3. Ginger and its constituents improve obesity-related inflammation

Inflammation is the mechanistic link between obesity, insulin resistance, and diabetes [31]. Several studies have revealed that the pro-inflammatory cytokines plasma tumor necrosis factor-α (TNF-α) and interleukin-6 (IL-6), are increased during a state of insulin resistance [32]. Thus, the inhibition of these inflammatory responses has been considered as a strategy to ameliorate insulin resistance and delay the development of type 2 diabetes. Kim *et al.* (2001) reported that salicylates improve fat-induced insulin resistance in skeletal muscle in rodent models of diabetes [33].

In clinical trials, Mahluji *et al.* (2013) revealed that oral supplementation of ginger for 2 months suppressed inflammation via reduction in TNF-α (proinflammatory cytokine) levels and hs-C-reactive protein (CRP, acute phase protein) in the blood of patients

with type 2 diabetes in comparison to a placebo group [34].

1.4. Summary

Ginger extract has protective effects against obesity and its complications. The mechanisms underlying the anti-obesity effects of ginger and its major compound 6-gingerol are thought to involve the inhibition of adipogenesis, amylase and pancreatic lipase activity, and the improvement of fatty acid oxidation. Recent studies have reported that ginger and 6-gingerol prevent insulin resistance and the development of type 2 diabetes by mitigating hyperglycemia, dyslipidemia, and inflammation. While 6-gingerol has been studied in depth (as it is generally accepted that 6-gingerol is the most prominent of the biologically active components), other bioactive constituents of ginger such as 8-gingerol, 10-gingerol and 6-shogaol, and gingerenone A have not been investigated in relation to obesity and its complications. Therefore, further research is necessary to determine the effects of alternative ginger components on dietary obesity and metabolic disorders.

1.5. Reference

1. Moreno-Indias, I. and F.J. Tinahones, Impaired Adipose Tissue Expandability and Lipogenic Capacities as Ones of the Main Causes of Metabolic Disorders. J Diabetes Res, 2015. 2015: p. 970375.
2. Morgen, C.S. and T.I. Sorensen, Obesity: global trends in the prevalence of overweight and obesity. Nat Rev Endocrinol, 2014. 10(9): p. 513-4.
3. Spiegelman, B.M. and J.S. Flier, Obesity and the regulation of energy balance. Cell, 2001. 104(4): p. 531-43.
4. Beltrán-Sánchez, H., et al., Prevalence and trends of Metabolic Syndrome in the adult US population, 1999-2010. Journal of the American College of Cardiology, 2013.
5. Pedersen, S.D., Metabolic complications of obesity. Best Practice & Research Clinical Endocrinology & Metabolism, 2013.

6. Després, J.-P. and I. Lemieux, Abdominal obesity and metabolic syndrome. Nature, 2006. 444(7121): p. 881-887.
7. Kammoun, H.L., M.J. Kraakman, and M.A. Febbraio, Adipose tissue inflammation in glucose metabolism. Rev Endocr Metab Disord, 2014. 15(1): p. 31-44.
8. White, B., Ginger: an overview. Am Fam Physician, 2007. 75(11): p. 1689-91.
9. Wang, W.H. and Z.M. Wang, [Studies of commonly used traditional medicine-ginger]. Zhongguo Zhong Yao Za Zhi, 2005. 30(20): p. 1569-73.
10. Hasan, H.A., et al., Chemical composition and antimicrobial activity of the crude extracts isolated from Zingiber officinale by different solvents. Pharm Anal Acta, 2012. 3(9): p. 184-9.
11. Bode, A.M. and Z. Dong, The Amazing and Mighty Ginger, in Herbal Medicine: Biomolecular and Clinical Aspects, I.F.F. Benzie and S. Wachtel-Galor, Editors. 2011: Boca Raton (FL).
12. Jo, J., et al., Hypertrophy and/or Hyperplasia: Dynamics of Adipose Tissue Growth. PLoS Comput Biol, 2009. 5(3): p. e1000324.

13. Rosen, E.D. and O.A. MacDougald, Adipocyte differentiation from the inside out. Nat Rev Mol Cell Biol, 2006. 7(12): p. 885-96.
14. Tzeng, T.F. and I.M. Liu, 6-gingerol prevents adipogenesis and the accumulation of cytoplasmic lipid droplets in 3T3-L1 cells. Phytomedicine, 2013. 20(6): p. 481-7.
15. Tzeng, T.F., C.J. Chang, and I.M. Liu, 6-gingerol inhibits rosiglitazone-induced adipogenesis in 3T3-L1 adipocytes. Phytother Res, 2014. 28(2): p. 187-92.
16. Saravanan, G., et al., Anti-obesity action of gingerol: effect on lipid profile, insulin, leptin, amylase and lipase in male obese rats induced by a high-fat diet. J Sci Food Agric, 2014. 94(14): p. 2972-7.
17. Tucci, S.A., E.J. Boyland, and J.C. Halford, The role of lipid and carbohydrate digestive enzyme inhibitors in the management of obesity: a review of current and emerging therapeutic agents. Diabetes Metab Syndr Obes, 2010. 3: p. 125-43.
18. Heck, A.M., J.A. Yanovski, and K.A. Calis, Orlistat, a new

lipase inhibitor for the management of obesity. Pharmacotherapy, 2000. 20(3): p. 270-9.

19. Homko, C.J., P. Cheung, and G. Boden, Effects of free fatty acids on glucose uptake and utilization in healthy women. Diabetes, 2003. 52(2): p. 487-91.
20. Kim, J.K., J.K. Wi, and J.H. Youn, Plasma free fatty acids decrease insulin-stimulated skeletal muscle glucose uptake by suppressing glycolysis in conscious rats. Diabetes, 1996. 45(4): p. 446-53.
21. Roden, M., et al., Mechanism of free fatty acid-induced insulin resistance in humans. J Clin Invest, 1996. 97(12): p. 2859-65.
22. Chang, C.J., et al., Regulation of lipid disorders by ethanol extracts from Zingiber zerumbet in high-fat diet-induced rats. Food Chemistry, 2012. 132(1): p. 460-467.
23. Fowler, M.J., Microvascular and macrovascular complications of diabetes. Clinical Diabetes, 2011. 29(3): p. 116-122.
24. Li, Y., et al., Preventive and Protective Properties of Zingiber officinale (Ginger) in Diabetes Mellitus, Diabetic Complications, and Associated Lipid and Other Metabolic

Disorders: A Brief Review. Evid Based Complement Alternat Med, 2012. 2012: p. 516870.

25. Li, Y., et al., Preventative effect of Zingiber officinale on insulin resistance in a high-fat high-carbohydrate diet-fed rat model and its mechanism of action. Basic Clin Pharmacol Toxicol, 2014. 115(2): p. 209-15.
26. Li, Y., et al., Gingerols of Zingiber officinale enhance glucose uptake by increasing cell surface GLUT4 in cultured L6 myotubes. Planta Med, 2012. 78(14): p. 1549-55.
27. Eleazu, C.O., et al., Ameliorative Potentials of Ginger (Z. officinale Roscoe) on Relative Organ Weights in Streptozotocin induced Diabetic Rats. Int J Biomed Sci, 2013. 9(2): p. 82-90.
28. Arablou, T., et al., The effect of ginger consumption on glycemic status, lipid profile and some inflammatory markers in patients with type 2 diabetes mellitus. Int J Food Sci Nutr, 2014. 65(4): p. 515-20.
29. Al-Noory, A.S., A.N. Amreen, and S. Hymoor, Antihyperlipidemic effects of ginger extracts in alloxan-induced diabetes and propylthiouracil-induced hypothyroidism

in (rats). Pharmacognosy Res, 2013. 5(3): p. 157-61.

30. Mahluji, S., et al., Effects of ginger (Zingiber officinale) on plasma glucose level, HbA1c and insulin sensitivity in type 2 diabetic patients. Int J Food Sci Nutr, 2013. 64(6): p. 682-6.
31. Shoelson, S.E., J. Lee, and A.B. Goldfine, Inflammation and insulin resistance. J Clin Invest, 2006. 116(7): p. 1793-801.
32. Dandona, P., A. Aljada, and A. Bandyopadhyay, Inflammation: the link between insulin resistance, obesity and diabetes. Trends in immunology, 2004. 25(1): p. 4-7.
33. Kim, J.K., et al., Prevention of fat-induced insulin resistance by salicylate. J Clin Invest, 2001. 108(3): p. 437-46.
34. Mahluji, S., et al., Anti-inflammatory effects of Zingiber officinale in type 2 diabetic patients. Advanced pharmaceutical bulletin, 2013. 3(2): p. 273.

Chapter 2.

Gingerenone A, an active diarylheptanoid present in ginger, suppresses adipogenesis and lipid accumulation in 3T3-L1 cells

Abstract

Adipogenesis and excessive lipid accumulation in mature adipocytes are the underlying cause of adipose tissue expansion. Ginger has been frequently used as an ingredient in nonprescription weight-loss products, but its bioactive properties have not been clearly investigated. In the present study, I compared the effects of several bioactive compounds present in ginger on adipogenesis and lipid accumulation in 3T3-L1 adipocytes. The anti-adipogenic and anti-lipogenic effects of gingerenone A (GA), a polyphenol compound, were superior in comparison to a number of other active compounds. GA dose-dependently suppressed intracellular lipid accumulation during adipogenesis of 3T3-L1 preadipocytes, consistent with a decrease in protein expression levels of peroxisome proliferator-activated receptor-γ (PPARγ), CCAAT/enhancer-binding protein α (C/EBPα) and fatty acid

synthase (FAS). Moreover, GA suppressed intracellular lipid accumulation dose-dependently in 3T3-L1 mature adipocytes, concomitant with a decrease in the expression levels of lipogenesis-related proteins such as FAS and sterol regulatory element–binding protein-1 (SREBP-1) and an increase in the expression levels of fatty acid oxidation-related proteins including peroxisome proliferator-activated receptor gamma coactivator 1α (PGC-1α) and carnitine palmitoyltransferase I (CPT1). These results indicate that GA attenuates adipogenic differentiation in 3T3-L1 preadipocytes and lipid accumulation in mature adipocytes, highlighting the potential therapeutic application of GA in preventing obesity.

2.1. Introduction

Recent studies have been conducted to identify novel substances possessing anti-adipogenic and anti-lipid accumulation properties in adipocytes to reduce the enlargement of adipose tissue mass responsible for obesity [1-3]. Adipogenesis, a process by which preadipocytes are differentiated into lipid-laden adipocytes, can be divided into initial and terminal differentiation steps [4, 5]. During the initial differentiation step, growth-arrested preadipocytes synchronously re-enter the cell cycle and undergo mitotic clonal expansion (MCE) [5]. Although the theory that MCE is a prerequisite for terminal differentiation remains controversial [6], many studies have found evidence supporting the notion that adipocyte differentiation can be inhibited via the modulation of MCE [2, 3, 7, 8]. In this step, transcription factors, peroxisome proliferator-activated receptor γ (PPARγ) and several members of

the CCAAT/enhancer-binding protein (C/EBP) family act as gene activators to transform preadipocytes into adipocytes [4, 5]. Of particular note, mRNA levels of PPARγ and C/EBPα are transiently increased by up to 8-12 fold. During the terminal differentiation step, the mRNA and protein levels of enzymes involved in triacylglycerol (TAG) synthesis and hydrolysis are significantly increased by activated transcriptional cascades [5]. Insulin sensitivity-related and adipokine synthesis-related markers are also significantly upregulated [9].

Adipocyte hypertrophy caused by increased lipid accumulation via an imbalance of fatty acid metabolism (which involves lipolysis, lipogenesis, and β-oxidation) provides a mechanistic link between obesity and metabolic disorders [10, 11]. Therefore, the modulation of fatty acid metabolism in adipocytes may provide a pivotal strategy for the prevention of metabolic disorders.

Ginger, *Zingiber officinale (Z. officinale)* Roscoe, has been historically used as a spice and traditional medicine in Korea, China, and India. Ginger possesses anti-obesity, anti-inflammatory,

hepatoprotective, anti-oxidant, anti-hyperlipidemic effects [12], and is composed of volatile oils (e.g. zingeberene, farnesene), non-volatile pungent components (e.g. gingerols, shogaols), and diarylheptanoid compounds (e.g. GA). Experimental evidence suggests that 6-gingerol (6G), a major bioactive component of ginger, has various pharmacological properties including anti-adipogenesis, anti-obesity, anti-insulin resistance effects [13-16]. Dugasani *et al*., compared the anti-oxidant and anti-inflammatory activities of several major non-volatile pungent compounds of ginger, 6G, 8-gingerol (8G), 10-gingerol (10G), and 6-shogaol (6S) *in vitro*, and determined the relative potencies as follows: 6S > 10G > 8G > 6G. Previous studies have shown that gingerenone A (GA), an active diarylheptanoid compound present in ginger, exerts anti-fungal, anti-oxidant, and anti-cancer effects [17, 18]. However, to date, there have been no studies reporting the effects of 6G, 8G, 10G, 6S, and GA on adipogenesis and lipid accumulation in 3T3-L1 cells.

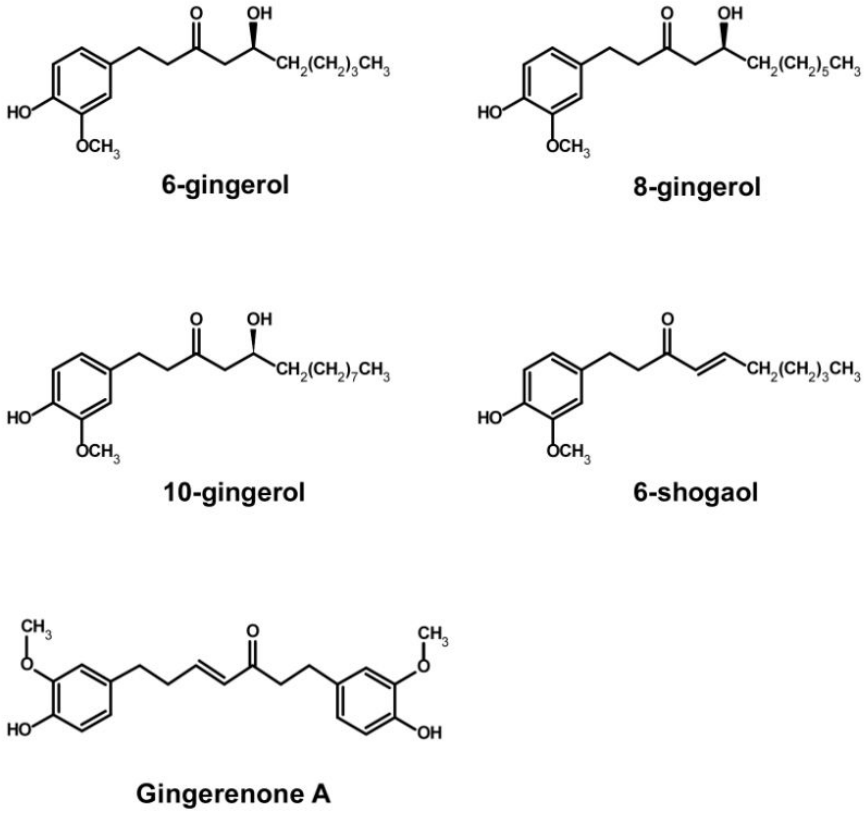

Figure 1. Chemical Structure of five bioactive compounds present in ginger

2.2. Materials and Methods

2.2.1. Chemicals and reagents

6G, 8G, 10G, and 6S were purchased from Sigma Chemical (St. Louis, MO). GA was synthesized from curcumin using a previously published procedure [19]. Dulbecco's modified Eagle's medium (DMEM) was purchased from Welgene (Daegu, Korea). Bovine calf serum (BCS), fetal bovine serum (FBS) and antibiotic-antimycotic were obtained from Life Technologies (Grand Island, NY). 3-isobutyl-methyl-xanthine (IBMX), dexamethasone (DEX), insulin, Oil red O (ORO) powder, and antibody against β-actin were purchased from Sigma Chemical (St. Louis, MO). Antibodies against sterol regulatory element–binding protein-1 (SREBP-1), carnitine palmitoyltransferase I (CPT1), and PPARγ were purchased from Santa Cruz Biotechnology (Santa Cruz, CA). Antibodies against fatty acid synthase (FAS) and C/EBPα, were obtained from Cell Signaling Biotechnology (Beverly, MA). Antibodies against peroxisome proliferator-activated receptor gamma coactivator 1α (PGC-1α) were obtained from Abcam (Cambridge, MA). The

lactate dehydrogenase (LDH) cytotoxicity detection kit was purchased from Takara Shuzo Co. (Otsu, Shiga, Japan).

2.2.2. Cell culture and differentiation

3T3-L1 cells were obtained from the American Type Culture Collection (ATCC, Manassas, VA) and maintained in DMEM containing 10% BCS and 1% antibiotic-antimycotic in a humidified atmosphere of 5% CO_2 at 37℃. After two days of culture, the cells reached monolayer confluence and the media was exchanged with DMEM supplemented with 10% FBS and an adipogenic cocktail including 0.5 mM IBMX, 1 μM DEX and 5 μg/ml insulin (MDI) for 2 days. The medium was then replaced with DMEM supplemented with 10% FBS and 5 μg/ml insulin, and the cells were cultured for a further 2 days. From Day 4, the cells were cultured in 10% FBS-DMEM for 2 additional days.

2.2.3. Cell viability and cytotoxicity

The effects of the ginger compounds on cell viability and cytotoxicity were determined by MTS and LDH release assays. Two

days post-confluence, the 3T3-L1 cells seeded in 96-well plate were treated with 10% FBS-DMEM medium containing MDI supplemented with the treatments at the indicated concentrations for 48 h. To determine the number of viable cells, 3-(4,5-dimethylthiazol-2-yl)-5-(3-carboxymethoxyphenyl)-2-4-sulfophenyl) -2H-tetrazolium salt (MTS) and phenazine methosulfate (PMS) mixture (CellTiter 96™ aqueous non-radioactive cell proliferation assay; Promega Corp.) was treated for 1 h at 37°C in a humidified 5% CO_2 atmosphere. Converted formazan was detected at 490 nm using a microplate reader (Molecular Devices, Menlo Park, CA). The cytotoxic effects of the ginger compounds were measured using an LDH detection kit (Otsu, Shiga, Japan). After centrifugation of the plate containing the cells at 250 x g for 10 min at room temperature, cell-free culture supernatants were transferred to clear 96-well plates. LDH activity was measured according to the manufacturer's protocol.

2.2.4. ORO staining

MDI-induced differentiated 3T3-L1 cells were fixed with

3.7% (v/v) paraformaldehyde in phosphate buffered saline (PBS) for 1 h at room temperature and then washed three times with PBS. Lipid droplets in the fixed cells were stained with ORO solution for 1 h. After ORO staining, the cells were washed three times with PBS. For the quantification of intracellular lipid content, the stained ORO was extracted with 2-propanol, and the absorbance was measured at 515 nm with a microplate reader (Molecular Devices, Menlo Park, CA).

2.2.5. Western blot analysis

Cultured 3T3-L1 cells in 6-cm dishes were treated as indicated for each experiment and the proteins were harvested by scraping with RIPA buffer (Cell Signaling Biotechnology). The protein concentration recovered from each sample was determined with a protein assay kit (Bio-Rad Laboratories, Hercules, CA). Proteins were separated by sodium dodecyl sulfate-polyacrylamide gel electrophoresis (SDS-PAGE) and transferred onto polyvinylidene difluoride membranes (Millipore, Marlborough, MA). The membranes were blocked with 5% skim milk and

incubated with the respective primary antibodies followed by incubation with horseradish peroxidase-conjugated secondary antibodies. A chemiluminescence detection kit (EZ-Western Super Enhancer Detection Kit, Daeil Lab, Seoul, Korea) was used to assess relative protein expression.

2.2.6. Glycerol release

3T3-L1 preadipocytes were differentiated in 24-well plates as described above. The cells were then treated with 6G, 8G, 10G or GA for 6 h. Next, the plates were centrifuged at 250 x g for 10 min at room temperature, before the cell-free culture supernatants were transferred to clear 96-well plates. Glycerol concentrations were measured using Free Glycerol Reagent (Sigma Chemical), according to the manufacturer's instructions.

2.2.7. Statistical analysis

Results are presented as means ± standard deviation (SD). Differences between the undifferentiated and differentiated control were assessed with unpaired Student's *t*-test. To compare the

differences between the differentiated groups, one-way analysis of variance (ANOVA) was used with Duncan's multiple range tests for *post hoc* analysis. Different letters indicate statistically significant differences between the MDI-treated groups. The data were statistically analyzed with IBM SPSS Statistics ver. 22.0 (IBM Co., Armonk, NY, USA) and $P < 0.05$ was used as the criteria for statistical significance.

2.3. Results

2.3.1. GA exerts the most potent inhibitory effect on MDI-induced adipogenesis in 3T3-L1 preadipocytes among five bioactive compounds present in ginger

I first investigated the effect of five bioactive ginger compounds, 6G, 8G, 10G, 6S, or GA, on adipogenesis in 3T3-L1 preadipocytes (Fig. 1). Post-confluent 3T3-L1 preadipocytes were stimulated with MDI to differentiate into mature adipocytes in the presence or absence of each ginger compound (40 μM) for 6 days. Photographic and quantitative assessments of intracellular lipid content by ORO staining revealed that GA had the most potent anti-adipogenic effect of the five ginger compounds tested at the same concentration (Fig. 2A and 2B). Compared to undifferentiated cells, the relative lipid levels of MDI-treated differentiated cells were significantly increased by 3.9-fold. MDI-induced lipid accumulation was most effectively reduced by GA at 40 μM, up to 76.0%, while

6G, 8G, 10G and 6S only caused reductions by 15.6%, 25.1%, 58.5% and 32.2% at 40 μM, respectively, in 3T3-L1 cells (Fig. 2B). In order to determine whether this anti-adipogenic effect was a result of cytotoxicity, I examined the cytotoxic effect of each ginger compound using an LDH release assay. The results showed that none of the compounds elicited cytotoxicity at 40 μM (Fig. 2C). Collectively, these results suggest that non-toxic concentrations of GA elicits the most potent anti-adipogenic effects among the five major non-volatile compounds present in ginger, tested *in vitro*.

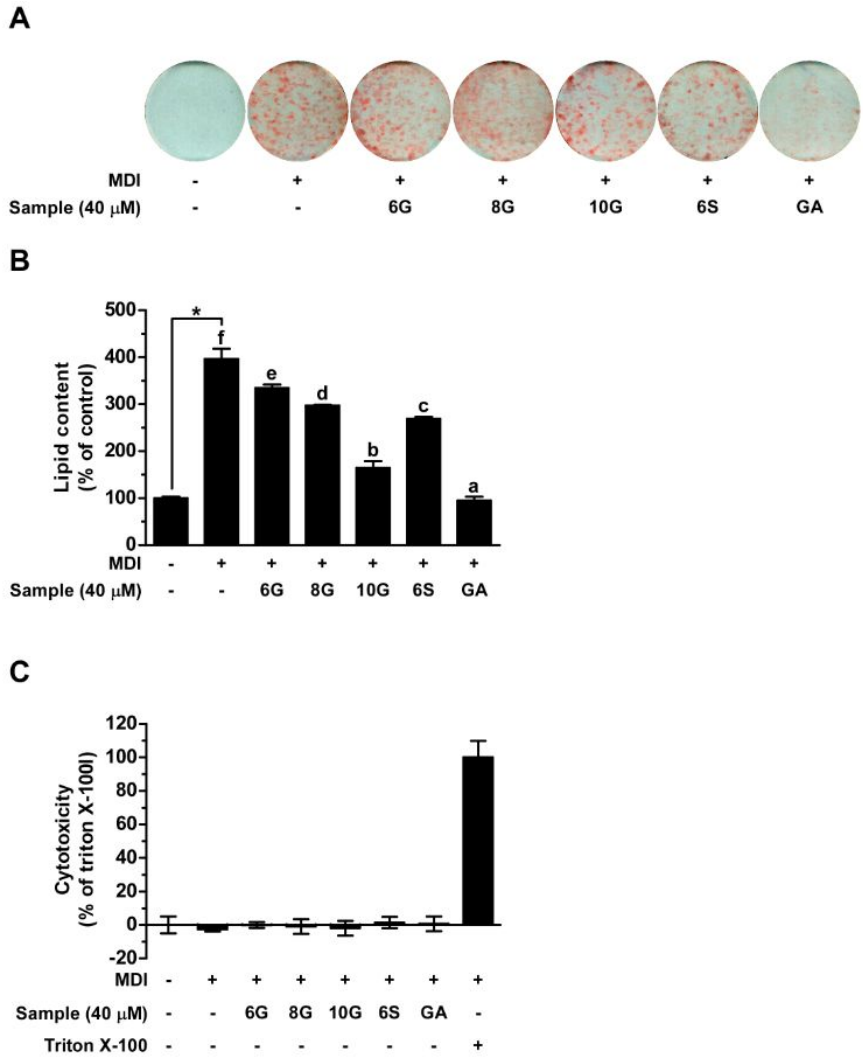

Figure 2. GA is the most potent anti-adipogenic agent among the five bioactive compounds present in ginger in 3T3-L1 preadipocytes. 3T3-L1 preadipocytes were stimulated with MDI to

differentiate into mature adipocytes with or without the indicated concentrations of the ginger compounds for 6 days. (A) The undifferentiated preadipocytes, MDI-induced adipocytes, and adipocytes differentiated with five bioactive compounds were subjected to ORO staining for visualization of lipid droplets. (B) Stained intracellular lipid droplets were extracted with 2-propanol and then quantified by measuring the absorbance at 515 nm. Lipid content for each group was expressed relative to that of undifferentiated cells (designated as 100%). (C) Post-confluent 3T3-L1 preadipocytes were incubated with MDI and five ginger compounds for 2 days, and the cytotoxicity of these cells was assessed by LDH release assay. Data are representative of 3 independent experiments, which are presented as means ± SD. Differences were considered significant at $P < 0.05$. * Significantly different between the undifferentiated control and differentiated control. Means with different letter (a, b, c, d, e, or f) are significantly different among MDI-treated groups.

2.3.2. GA suppresses adipogenesis and down-regulates expression levels of adipogenic and lipogenic proteins

To examine the effect of various concentrations of GA on adipogenesis, post-confluent 3T3-L1 preadipocytes were treated with MDI supplemented with different concentrations of GA (10, 20 and 40 μM) for 6 days. In this experiment, I used 6G as a positive control due to its anti-adipogenic effect on 3T3-L1 preadipocytes. The cells were then stained with ORO to measure intracellular lipid contents. Visualized and quantitative data demonstrated that treatment with GA reduced lipid accumulation more effectively than 6G, especially at 40 μM (Fig. 3A and 3B).

Consistent with these results, protein expression levels of adipogenic transcription factors such as PPARγ and C/EBPα in cells treated with GA at concentrations of 20 and 40 μM were lower than those for control cells differentiated for 6 days (Fig. 3C). Furthermore, GA treatment abolished expression of the lipogenic protein FAS at concentrations of 20 and 40 μM (Fig. 3C). Taken

together, I conclude that GA inhibits adipogenesis of 3T3-L1 preadipocytes by reducing the expression levels of adipogenic and lipogenic proteins.

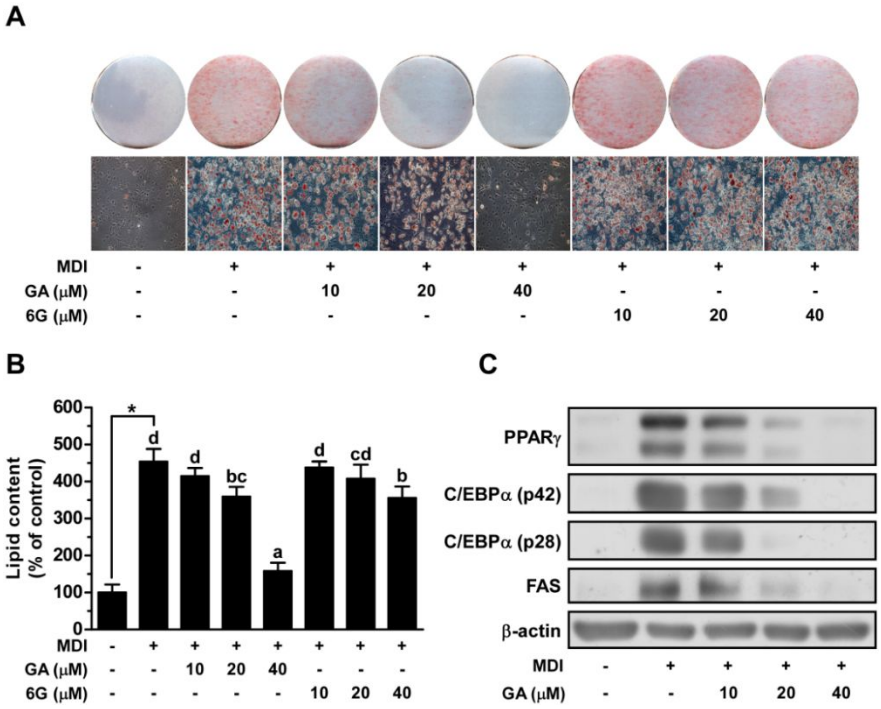

Figure 3. GA inhibits adipogenesis and down-regulates expression levels of adipogenic and lipogenic proteins dose-dependently. (A-B) 3T3-L1 preadipocytes were treated with GA and 6G at various concentrations during adipogenesis. After 6 days of differentiation, these cells were subjected to ORO staining for visualization and

quantification of intracellular lipid droplets. The data were expressed as means ± SD. * Significantly different between undifferentiated control and differentiated control. Different letters indicate statistically significant differences among the differentiated groups. Differences were considered significant at $P < 0.05$. (C) Protein levels of PPARγ, C/EBPα, and FAS were examined in 3T3-L1 cells after 6 days of differentiation as determined by Western blot analysis. β-actin was used as loading control.

2.3.3. GA suppresses lipid accumulation in 3T3-L1 mature adipocytes

Next, I evaluated the effect of the ginger bioactive compounds on adipocyte hypertrophy. Matured 3T3-L1 cells were incubated for 4 days and supplemented with the ginger compounds (40 μM) (Fig. 1). GA decreased lipid accumulation in mature adipocytes, in contrast to the other compounds that had no effect on lipid accumulation across all non-toxic concentrations tested (Fig. 4A and 4C).

In the adipocytes, reduction of lipid droplets, which are mainly composed of a neutral lipid (TAG), can be caused by elevated lipolysis, defined as the hydrolysis of TAG to generate fatty acids (FAs) and glycerol. I therefore next chose to assess the lipolytic activity of ginger compounds by the measurement of released glycerol contents in the medium. The results showed that 6G, 8G, and GA significantly decreased glycerol release when

compared to the control group (Fig. 4B). Of particular note, GA elicited the most potent inhibitory effect on lipolysis. I also found that the inhibitory effect of GA on intracellular lipid accumulation was dose-dependent (10, 20 and 40 μM; 90, 84.6, and 77%; % of the control) (Fig. 5A). I then investigated whether GA may be regulating other fatty acid metabolic processes such as lipogenesis or fatty acid oxidation. The protein expression levels of SREBP-1 and FAS (lipogenesis markers) were decreased, and the protein expression of PGC-1α and CPT-1 (fatty acid oxidation markers) was increased after treatment with GA (Fig. 5B and 5C). These results indicate that GA suppresses adipocyte lipid accumulation via the regulation of fatty acid metabolism.

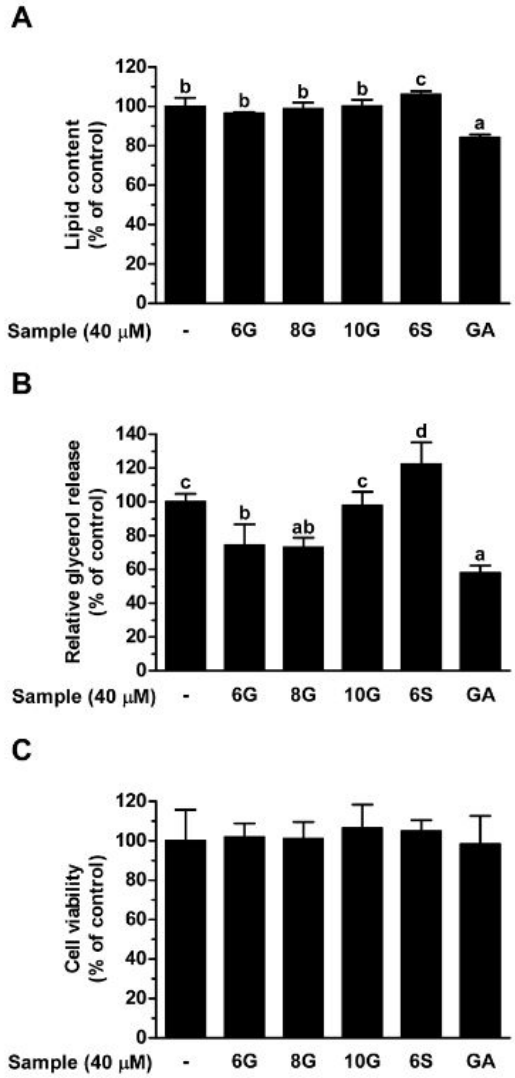

Figure 4. GA has the most potent inhibitory effect on lipid accumulation in mature adipocytes. 3T3-L1 preadipocytes were differentiated into adipocytes. Fully differentiated adipocytes were

treated with ginger compounds (6G, 8G, 10G, 6S, and GA) at 40 μM for 4 days, and cells were subjected to ORO staining of intracellular lipid accumulation. (A) Quantification of ORO staining and (B) the relative glycerol release. (C) Effect of GA on the viability of 3T3-L1 mature adipocytes by MTS assay. Data represent means ± SD, and values shown as percentages relative to control. To compare the differences among the groups, one-way ANOVA was used with Duncan's multiple rage tests for *post hoc* analysis. Different letters indicate statistically significant differences at $P < 0.05$

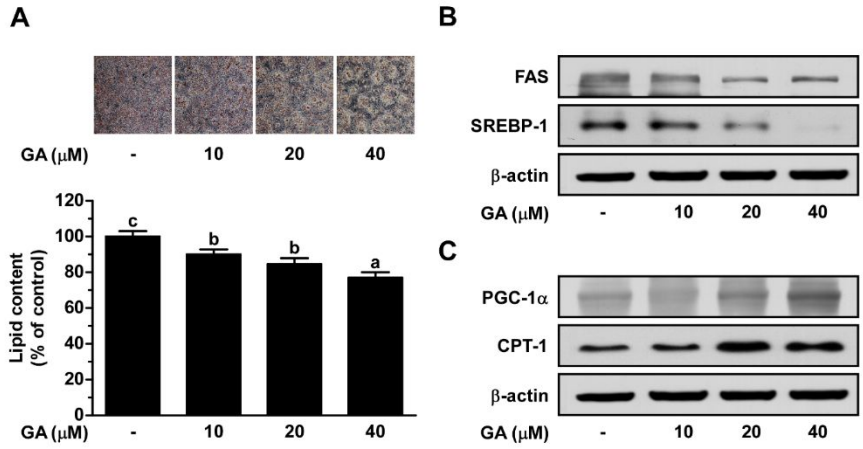

Figure 5. GA suppresses lipid accumulation of mature adipocytes by regulating the expression of lipogenesis- and fatty acid oxidation-related proteins. (A) Representative optical image (upper lane) and relative intracellular lipid content of 3T3-L1 adipocytes. Data represent means ± SD. One-way ANOVA was used with Duncan's multiple rage tests for *post hoc* analysis. Different letters indicate statistically significant differences at $P < 0.05$. Western blot analyses of (B) lipogenesis-related proteins (SERBP-1 and FAS) and (C) fatty acid oxidation-related proteins (PGC-1α and CPT-1). β-actin was measured as loading control.

2.4. Discussion

Ginger has been reported to exert anti-obesity effects in chemical- and high-fat diet (HFD)-induced obese mice [20-22]. 6G, a bioactive compound found in ginger, has been considered as a key factor for the anti-obesity effect of ginger because it is known to activate transient receptor potential vanilloid-1 (TRPV1) [23]. A TRPV1 agonist, capsaicin, was found to exert anti-adipogenic and anti-obesity effects *in vitro* and *in vivo* [24]. Likewise, 6G prevents adipogenesis and reduces intracellular lipid droplets in 3T3-L1 cells, and mitigates body weight gain in mice fed on an HFD [15, 25]. While 6G has been studied in depth, other bioactive ingredients present in ginger such as 8G, 10G and 6S, and GA have not been previously been studied in relation to obesity.

Hence, in the present study, I first compared the anti-adipogenic effects of the ginger compounds. Interestingly, GA exhibited the most potent anti-adipogenic activity among the five ginger compounds tested on adipogenesis in 3T3-L1 preadipocytes. Furthermore, I observed that GA was able to reduce the protein expression levels of FAS as well as PPARγ and C/EBPα during this

period. FAS is a lipogenic enzyme that is involved in the synthesis and storage of triglycerides [26]. Liu LH *et al*., found that C75 (a FAS inhibitor) inhibited adipogenesis via down-regulation of PPARγ mRNA [27].

Next, I evaluated the effect of the ginger compounds on fully differentiated 3T3-L1 adipocytes, which contain densely accumulated lipid droplets. Consistent with the anti-adipogenic effects observed, GA elicited the most potent inhibitory effect on intracellular lipid accumulation. I had initially expected that the reduced lipid content caused by GA treatment was a result of increased lipolytic activity, but instead GA significantly inhibited the secretion of glycerol into the media. GA inhibited the expression levels of lipogenesis-related proteins, while it increased those of free fatty acid oxidation-related proteins. Several studies have reported that enhanced energy expenditure based on β-oxidation in adipose tissue helps to improve obesity and metabolic disorders in rodents and humans [28-30]. This requires further investigation to identify the mechanisms responsible for how GA regulates fatty acid metabolism.

In conclusion, GA inhibits not only adipogenesis of 3T3-L1 preadipocytes but also lipid accumulation of 3T3-L1 mature adipocytes. Taken together, these findings suggest that GA has significant potential to prevent obesity and metabolic disorders. However, further studies are necessary to fully understand the effect of GA on diet-induced obesity.

2.5. Reference

1. Cheong, L.Y., et al., Hirsutenone Directly Targets PI3K and ERK to Inhibit Adipogenesis in 3T3-L1 Preadipocytes. J Cell Biochem, 2015.
2. Min, S.Y., et al., Cocoa polyphenols suppress adipogenesis in vitro and obesity in vivo by targeting insulin receptor. Int J Obes (Lond), 2013. 37(4): p. 584-92.
3. Shin, S.H., et al., Caffeic acid phenethyl ester, a major component of propolis, suppresses high fat diet-induced obesity through inhibiting adipogenesis at the mitotic clonal expansion stage. J Agric Food Chem, 2014. 62(19): p. 4306-12.
4. Rosen, E.D. and O.A. MacDougald, Adipocyte differentiation from the inside out. Nat Rev Mol Cell Biol, 2006. 7(12): p. 885-96.
5. Tang, Q.Q., T.C. Otto, and M.D. Lane, Mitotic clonal expansion: a synchronous process required for adipogenesis. Proc Natl Acad Sci U S A, 2003. 100(1): p. 44-9.
6. Qiu, Z., et al., DNA synthesis and mitotic clonal expansion is

not a required step for 3T3-L1 preadipocyte differentiation into adipocytes. J Biol Chem, 2001. 276(15): p. 11988-95.

7. Seo, S.G., et al., A metabolite of daidzein, 6,7,4'-trihydroxyisoflavone, suppresses adipogenesis in 3T3-L1 preadipocytes via ATP-competitive inhibition of PI3K. Mol Nutr Food Res, 2013. 57(8): p. 1446-55.
8. Kwon, J.Y., et al., An inhibitory effect of resveratrol in the mitotic clonal expansion and insulin signaling pathway in the early phase of adipogenesis. Nutr Res, 2012. 32(8): p. 607-16.
9. Gregoire, F.M., Adipocyte differentiation: from fibroblast to endocrine cell. Exp Biol Med (Maywood), 2001. 226(11): p. 997-1002.
10. Tanaka, T., H. Masuzaki, and K. Nakao, [Adipocyte dysfunction and insulin resistance]. Nihon Rinsho, 2006. 64 Suppl 9: p. 149-57.
11. Kloting, N. and M. Bluher, Adipocyte dysfunction, inflammation and metabolic syndrome. Rev Endocr Metab Disord, 2014. 15(4): p. 277-87.
12. Bode, A.M. and Z. Dong, The Amazing and Mighty Ginger, in

Herbal Medicine: Biomolecular and Clinical Aspects, I.F.F. Benzie and S. Wachtel-Galor, Editors. 2011: Boca Raton (FL).

13. Saravanan, G., et al., Anti-obesity action of gingerol: effect on lipid profile, insulin, leptin, amylase and lipase in male obese rats induced by a high-fat diet. J Sci Food Agric, 2014. 94(14): p. 2972-7.
14. Tzeng, T.F., C.J. Chang, and I.M. Liu, 6-gingerol inhibits rosiglitazone-induced adipogenesis in 3T3-L1 adipocytes. Phytother Res, 2014. 28(2): p. 187-92.
15. Tzeng, T.F. and I.M. Liu, 6-gingerol prevents adipogenesis and the accumulation of cytoplasmic lipid droplets in 3T3-L1 cells. Phytomedicine, 2013. 20(6): p. 481-7.
16. Li, Y., et al., Preventative effect of Zingiber officinale on insulin resistance in a high-fat high-carbohydrate diet-fed rat model and its mechanism of action. Basic Clin Pharmacol Toxicol, 2014. 115(2): p. 209-15.
17. Endo, K., E. Kanno, and Y. Oshima, Structures of Antifungal Diarylheptenones, Gingerenone-a, Gingerenone-B, Gingerenone-C and Isogingerenone-B, Isolated from the

Rhizomes of Zingiber-Officinale. Phytochemistry, 1990. 29(3): p. 797-799.

18. Yang, L., et al., [Antioxidative and cytotoxic properties of diarylheptanoids isolated from Zingiber officinale]. Zhongguo Zhong Yao Za Zhi, 2009. 34(3): p. 319-23.
19. Venkateswarlu, S., et al., Synthesis of gingerenone-A and hirsutenone. Indian Journal of Chemistry Section B-Organic Chemistry Including Medicinal Chemistry, 2001. 40(6): p. 495-497.
20. Goyal, R.K. and S.V. Kadnur, Beneficial effects of Zingiber officinale on goldthioglucose induced obesity. Fitoterapia, 2006. 77(3): p. 160-3.
21. Han, L.K., et al., [Antiobesity actions of Zingiber officinale Roscoe]. Yakugaku Zasshi, 2005. 125(2): p. 213-7.
22. Nammi, S., S. Sreemantula, and B.D. Roufogalis, Protective effects of ethanolic extract of Zingiber officinale rhizome on the development of metabolic syndrome in high-fat diet-fed rats. Basic Clin Pharmacol Toxicol, 2009. 104(5): p. 366-73.
23. Iwasaki, Y., et al., A nonpungent component of steamed ginger-

-[10]-shogaol--increases adrenaline secretion via the activation of TRPV1. Nutr Neurosci, 2006. 9(3-4): p. 169-78.

24. Zhang, L.L., et al., Activation of transient receptor potential vanilloid type-1 channel prevents adipogenesis and obesity. Circ Res, 2007. 100(7): p. 1063-70.
25. Okamoto, M., et al., Synthesis of a new [6]-gingerol analogue and its protective effect with respect to the development of metabolic syndrome in mice fed a high-fat diet. J Med Chem, 2011. 54(18): p. 6295-304.
26. Student, A.K., R.Y. Hsu, and M.D. Lane, Induction of fatty acid synthetase synthesis in differentiating 3T3-L1 preadipocytes. J Biol Chem, 1980. 255(10): p. 4745-50.
27. Liu, L.H., et al., Effects of a fatty acid synthase inhibitor on adipocyte differentiation of mouse 3T3-L1 cells. Acta Pharmacol Sin, 2004. 25(8): p. 1052-7.
28. Flachs, P., et al., Stimulation of mitochondrial oxidative capacity in white fat independent of UCP1: a key to lean phenotype. Biochim Biophys Acta, 2013. 1831(5): p. 986-1003.
29. Qi, L., et al., TRB3 links the E3 ubiquitin ligase COP1 to lipid

metabolism. Science, 2006. 312(5781): p. 1763-6.

30. Rosen, E.D. and B.M. Spiegelman, Adipocytes as regulators of energy balance and glucose homeostasis. Nature, 2006. 444(7121): p. 847-53.

Chapter 3.

Gingerenone A suppresses high-fat diet-induced obesity in mice

Abstract

The primary factors contributing to the growing obesity epidemic are thought to include genetic susceptibility, excessive food intake, and lack of physical activity. Excessive caloric intake results in an enlarged body fat mass, which (when sustained) has a negative overall effect on health. Here, I investigated the effect of gingerenone A (GA), a polyphenol present in ginger, on high-fat diet (HFD)-induced obesity in C57BL/6 mice. I observed that supplementation with 50 mg/kg of GA suppressed body weight gain induced by HFD feeding via a reduction in adipose tissue mass with no change to circulating free fatty acids (FFAs) and ectopic lipid accumulation in the central organ. GA regulated fatty acid metabolism in a positive manner (e.g. GA increased fatty acid oxidation and decreased lipogenesis) to reduce adipose tissue mass. Together, these results suggest that GA has therapeutic potential for the prevention of diet-induced obesity.

3.1. Introduction

The growing epidemic of obesity is thought to be caused by genetic susceptibility and environmental factors such as excessive food intake and a lack of physical activity. Obesity is characterized by an excessively enlarged body fat mass, and can have a negative effect on health [1].

White adipose tissue (WAT) has been characterized as a storage depot for excessively loaded energy in the body [2]. Extra energy is stored as neutral lipids (triacylglycerols (TAG) and cholesterol esters (CE)) in adipocyte lipid droplets. The lipids originate from ingested TAG in food and/or endogenous synthesis of fatty acids (de novo lipogenesis) [3]. When the body requires energy, stored fat is degraded into free fatty acids (FFA) and glycerol, a process referred to as lipolysis [3, 4]. Adipose triglyceride lipase (ATGL) and hormone-sensitive lipase (HSL) are the major enzymes responsible for adipose tissue lipolysis. ATGL initially degrades TAG to produce diacylglycerol (DAG) and FFA [4]. HSL then degrades DAG to release two free fatty acids (FFAs) and glycerol. Phosphorylation of HSL (p-HSL) at the Serine 565

residue by AMP-activated protein kinase (AMPK) impairs lipolysis by preventing the phosphorylation of the PKA-targeted Serine 563 and Serine 660 residues [5]. The FFAs are then metabolized to produce energy sources through mitochondrial β-oxidation [4]. Several studies have reported that enhanced energy expenditure based on β-oxidation via lipolysis in WAT helps to improve obesity and metabolic disorders in rodents and humans [6-8]. Moreover, obese subjects have not only greater quantities of stored TAG, but also show a lower lipid turnover rate than non-obese subjects [9].

AMPK, a major energy sensor in the cell, is activated when energy demands increase [10]. Activated AMPK inhibits anabolic pathways (such as gluconeogenesis, protein synthesis) and enhances catabolic pathways (such as glycolysis, fatty acid oxidation) [10]. Although these roles for AMPK in muscle and liver tissue are well known, there have also been several studies proposing that activated AMPK influences obesity and insulin resistance via enhancement of β-oxidation and inhibition of lipogenesis in WAT [6, 11]. Previous studies have suggested that natural compounds that are beneficial in the treatment of obesity and metabolic disorders increase AMPK

activity [11-13].

Recent efforts are being made to identify novel dietary bioactive substances that can be used to reduce the incidence and severity of obesity [14]. To date, ginger, a major ingredient in nonprescription weight-loss products, has been commonly used for preventing obesity [15], but the molecular mechanisms of action for its active compounds have not been clearly elucidated. In Chapter 2, I reported that gingerenone A (GA) has the greatest anti-adipogenic effect among the ginger-derived active compounds tested *in vitro*. In this study I further investigated the effect of GA on diet-induced obesity and the underlying molecular mechanisms *in vivo*.

3.2. Materials and Methods

3.2.1. Chemicals and reagents

GA was synthesized from curcumin using a previously published procedure [16]. Antibody against sterol regulatory element–binding protein-1 (SREBP-1) was purchased from Santa Cruz Biotechnology (Santa Cruz, CA). Antibodies against ATGL, p-HSL (Ser565), HSL, fatty acid synthase (FAS), phospho-AMPK α (p-AMPKα) (Thr172), AMPKα, phospho-acetyl-CoA carboxylase (p-ACC) (Ser79), and ACC were obtained from Cell Signaling Biotechnology (Beverly, MA). Antibodies against glyceraldehyde-3-phosphate dehydrogenase (GAPDH) were purchased from Sigma Chemical (St. Louis, MO).

3.2.2. Experimental animals and diets

All experiments were approved by the Seoul National University Animal Experiments Ethics Committee. Six-week-old male C57BL/6 mice were purchased from Japan SLC Inc. (Hamamatsu, Shizuoka, Japan) and acclimated for 1 week before

the study, with free access to chow and water. A total of 47 mice were randomly assigned to the following four groups: standard diet (SD, D12450B Rodent Diet with 10 kcal% fat; Research Diets, Inc., NJ, USA) (12 mice), high-fat diet (HFD, D12492 Rodent Diet with 60 kcal% fat; Research Diets) (12 mice), HFD plus 50 mg/kg body weight GA (HFD-GA50; 12 mice), or HFD plus 10 mg/kg body weight GA (HFD-GA10; 11 mice). The diet formulations were purchased from Research Diets, Inc. (New Brunswick, NJ) and provided in the form of pellets for 15 weeks. GA was dissolved in polyethylene glycol (PEG) 200 and introduced to the animals by oral gavage every day. After 15 weeks of treatment, mice were sacrificed under intraperitoneal Zoletil/Rompun anesthesia after an overnight fast, and all efforts were made to minimize suffering. Blood samples were collected from the heart chambers. Following blood collection, several tissue samples were promptly removed and rinsed with PBS and weighted. Epididymal adipose tissue (EWAT) was snap-frozen in liquid nitrogen and stored at -80℃ for RNA and protein analysis.

3.2.3. Serum and liver biochemical analyses

Blood samples were collected in serum separator tubes (Becton Dickinson; Franklin Lakes, NJ) and centrifuged at 1,100 x g for 20 min. TG and total cholesterol (TC) levels in the serum and liver were measured with a commercial kit (Asan Pharmaceutical Co., Seoul, Korea). Serum FFAs were determined using a Wako NEFA C test kit (Wako Chemicals, Osaka, Japan). Serum insulin was determined by ELISA (ALPCO Diagnostics, Salem, NH)

3.2.4. Hematoxylin and eosin staining and adipocyte cell size assessment

Paraffin sections of formalin-fixed EWATs were stained with hematoxylin and eosin (H&E) for morphological evaluation. The area of each adipocyte was quantified using Image J software (National Institutes of Health).

3.2.5. Quantitative real-time polymerase chain reaction analysis

Total RNA was extracted from EWATs with an Ambion® RNA isolation kit (Life Technologies, Gaithersburg, MD). cDNA

was synthesized with a PrimeScript™ 1st strand cDNA Synthesis Kit (Takara, Kyoto, Japan) and quantitative real-time polymerase chain reaction (qRT-PCR) was conducted using specific primers and SYBR Green Master Mix (BioRad, Hercules, CA) with a Bio-Rad CFX96 real-time PCR detection system (BioRad, Hercules, CA). The forward and reverse primers for each transcript were as follows: *ppara*: AGG CTG TAA GGG CTT CTT TCG and GGC ATT TGT TCC GGT TCT TC; *acsl1*: TGG GGT GGA AAT CAT CAG CC and CAC AGC ATT ACA CAC TGT ACA ACG G; *cpt2*: GAA GAA GCT GAG CCC TGA TG and GCC ATG GTA TTT GGA GCA CT; *ppargc1a*: GAA AGG GCC AAA CAG AGA GA and GTA AAT CAC ACG GCG CTC TT; *nrf1*: TTA CTC TGC TGT GGC TGA TGG and CCT CTG ATG CTT GCG TCG TCT; *tfam* AAT GTG GAG CGT GCT AAA AG and AGC TGT TCT GTG GAA AAT CG; *Gapdh*: CAA GGA GTA AGA AAC CCT GGA CC and CGA GTT GGG ATA GGG CCT CT.

3.2.6. Immunoblotting

EWATs were lysed with RIPA buffer (Cell Signaling

Biotechnology) and centrifuged (24,100 x g, 4°C, 10 min) in order to collect supernatants separately to the layer of fat. The protein extracts were loaded onto sodium dodecyl sulfate-polyacrylamide gel electrophoresis (SDS-PAGE) gels and transferred to polyvinylidene fluoride (PVDF) membranes (Millipore, Marlborough, MA). The membranes were blocked with 5% skim milk and incubated with specific primary antibodies followed by incubation with horseradish peroxidase (HRP)-conjugated secondary antibodies. Protein bands were visualized using a chemiluminescence detection kit (Amersham Pharmacia Biotech; Piscataway, NJ).

3.2.7. Statistical analysis

Data are expressed as means ± standard error of mean (SEM). The differences between the SD-fed and HFD-fed groups were assessed via Student's *t*-test. HFD-fed group results were compared using one-way analysis of variance (ANOVA) with *post hoc* Duncan's test or two-way ANOVA followed by a Bonferroni *post hoc* test. A probability value of $P < 0.05$ was used as the

criterion for statistical significance.

3.3. Results

3.3.1. GA attenuates HFD-induced body weight gain in mice

To investigate the anti-obesity effect of GA *in vivo*, I administered GA orally (10, 50 mg/kg) to C57BL/6 mice on HFD for 15 weeks. The group administered with 50 mg/kg GA registered lower body weights (30.82 ± 0.50 g) than the HFD group (33.87 ± 0.88 g) at 15 weeks ($P < 0.001$; Fig. 1A). Treatment with the lower dose of GA (HFD-GA10), however, did not cause a significant change in body weight (34.91 ± 0.68 g) over 15 weeks (Fig. 1A). Notably, the final body weight of the HFD-GA50 mice was not significantly different from the mice fed on SD (Fig. 1B). Although daily food and calorie intakes were not different between the HFD-fed (2.14 ± 0.08 g/mouse/day; 11.20 ± 0.39 kcal/mouse/day) and HFD-GA groups (10 mg/kg, 2.16 ± 0.08 g/mouse/day, 11.33 ± 0.40 kcal/mice/day; 50 mg/kg, 2.17 ± 0.06 g/mouse/day, 11.52 ± 0.36 kcal/mice/day) (Fig. 1C and Fig. 1D), the food efficiency ratio

(FER), which was calculated as previously described [17], was significantly lower in the HFD-GA50 group than in the HFD group by up to 30% (Fig. 1E). Collectively, these results suggest that GA 50 mg/kg supplementation attenuates diet-induced obesity without having a significant effect on food intake.

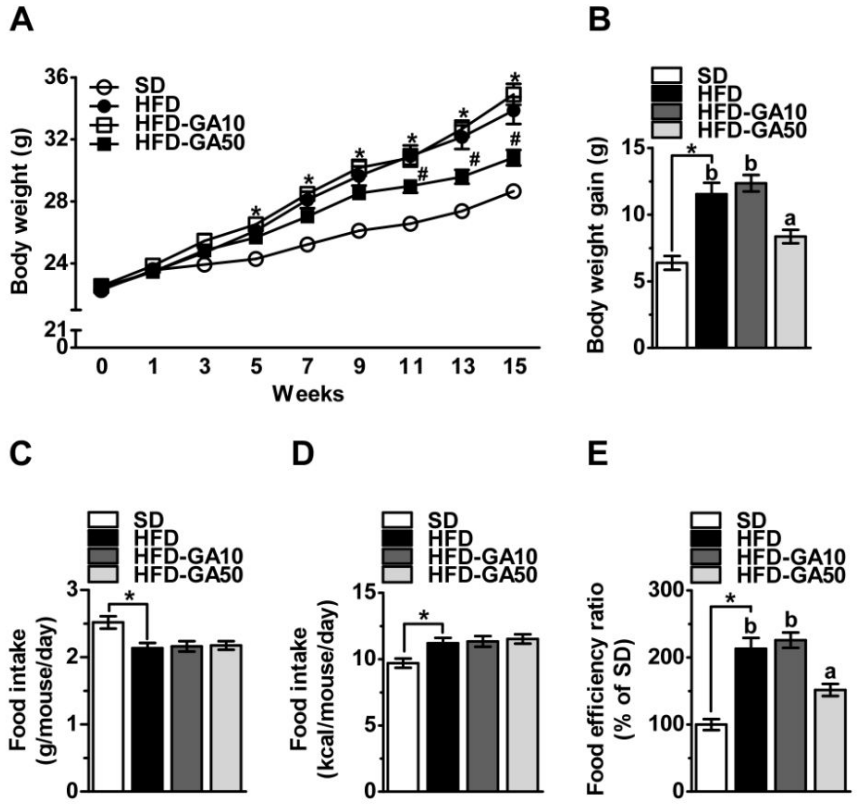

Figure 1. GA administration suppresses HFD-induced body weight gain in mice. Six-week-old male C57BL/6 mice were fed a SD (12 mice), HFD (12 mice), HFD + GA 10 mg/kg (HFD-GA10; 11 mice), or HFD + GA 50 mg/kg (HFD-GA50; 12 mice) for 15 weeks. GA was given daily by oral gavage in PEG 200 solution. Mice in the SD and HFD group were gavaged with vehicle only. (A) Body weight curves and (B) body weight gain over 15 weeks. (C) Food intake

(g/mouse/day) and (D) energy intake (kcal/mouse/day) was calculated once a week. (E) Food efficiency ratio [body weight gain (g)/food intake (g) for 15 weeks] was calculated and the control levels were set to 100%. The time course values of change in body weight were analyzed by two-way ANOVA followed by a Bonferroni *post hoc* test (*$P < 0.05$ HFD vs. SD; $^{\#}P < 0.05$ GA-treatment groups vs. HFD). Unpaired Student's *t*-test was used to detect statistically significant differences between SD and HFD group (*$P < 0.05$). Then, one-way ANOVA was used with Duncan's multiple rage tests for *post hoc* analysis to compare the differences among the three HFD groups. Different letters indicate statistically significant differences. Differences were considered significant at $P < 0.05$

3.3.2. GA reduces HFD-induced enlarged fat mass by reducing adipocyte size

Enlarged fat mass is a major aspect of diet-induced obesity. I sought to determine whether the decrease in body weight gain was associated with a decrease in fat mass. Consistent with the photographic results (Fig. 2A), total fat mass (sum of inguinal and visceral fat mass) of HFD-GA50 mice was reduced by ~33%, but not in HFD-GA10 mice, which was accompanied by a decrease of ~40% and ~32% in the inguinal and visceral fat masses of HFD-GA50, respectively, compared with the HFD mice (Fig. 2B-2D). The weight of visceral fat (epididymal, mesenteric, and retroperitoneal) was significantly lower in the HFD-GA50 group than in the HFD group (Fig. 2E-2G). Perineal fat weight in the HFD-GA50 group also tended to be lower than the HFD group.

In order to determine whether the reductions in fat mass were correlated with adipocyte size, I performed histological analyses of fixed EWAT and quantified adipocyte sizes. The results revealed that adipocytes from HFD-fed mice were significantly

larger than SD-fed mice up to 2-fold, however, the adipocytes from HFD-GA50 were significantly smaller than the adipocytes from the HFD group by 46% (Fig. 3A and Fig. 3B). Analyses of adipocyte size distribution in EWAT revealed that HFD feeding resulted in a significant shift toward larger adipocytes, whereas treatment of HFD-fed mice with GA 50 mg/kg showed a negation of this shift and a restored normal distribution profile for adipocyte size (Fig. 3C). Taken together, these results suggest that GA supplementation decreases HFD-induced fat mass gain by reducing adipocyte size.

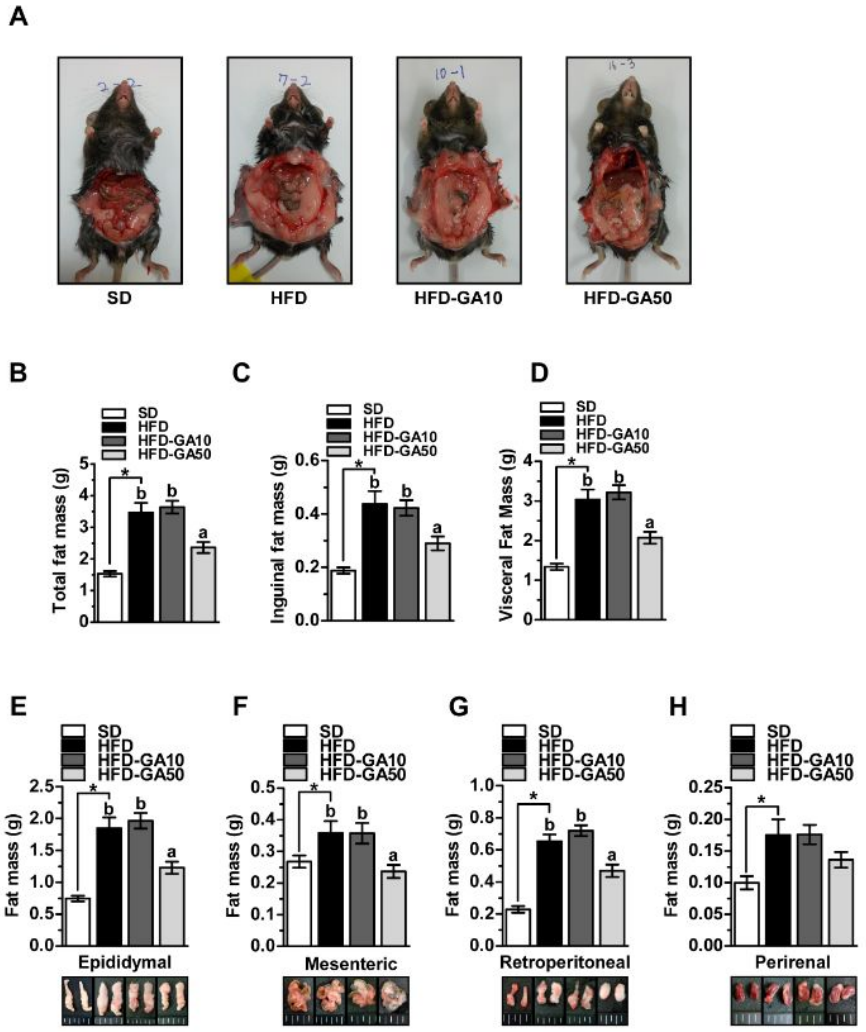

Figure 2. GA treatment reduces adipose tissue mass. HFD with or without GA administration for 15 weeks, and mice were sacrificed. (A) Representative abdominal view. (B) Total fat mass, (C) inguinal

fat mass, and (D) visceral fat mass. (E-H) Weights of various visceral fat pads. Each fat mass were presented as means ± SEM. * Significant difference between SD and HFD group. Different letters indicate statistically significant differences between the HFD-treated groups. Differences were considered significant at $P < 0.05$.

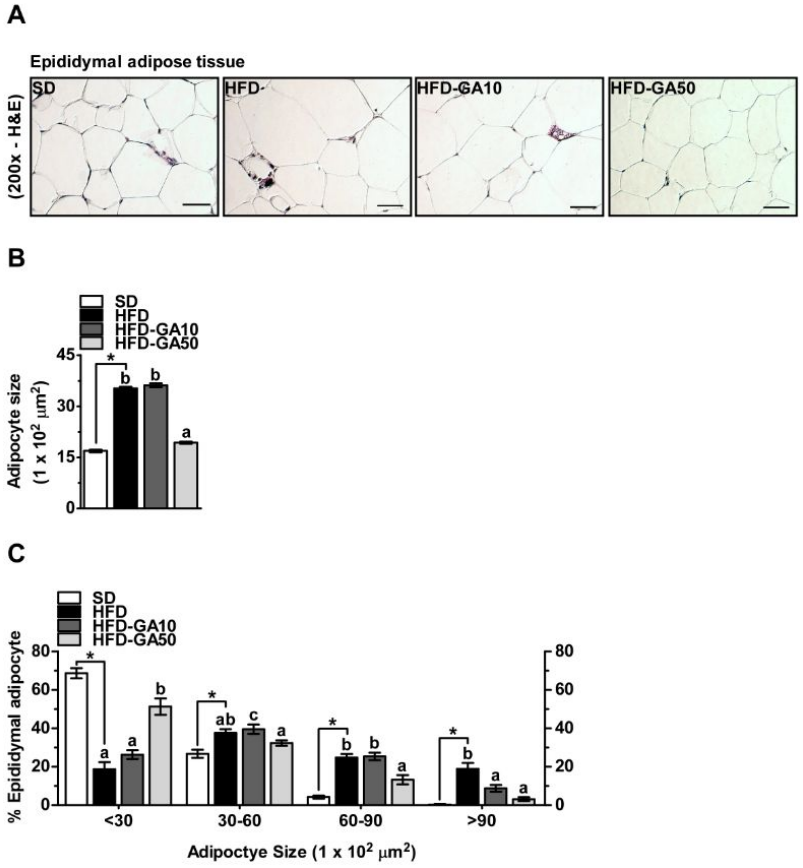

Figure 3. GA treatment reduces adipocyte size. (A) Sections of EWAT were stained with H&E. Representative images are shown. Scale bar, 200 μm. (B) Adipocyte size area and (C) adipocyte size distribution of EWAT. Data are expressed as means ± SEM. * Significant differences between SD and HFD group. Different letters indicate statistically significant differences between the HFD-treated groups. Differences were considered significant at $P <$

0.05

3.3.3. GA decreases circulating FFA levels

I next evaluated serum and liver lipid concentrations because a decrease in adipose tissue mass can trigger lipodystrophy, an abnormal state of adipose tissue. Lipodystrophy can lead to ectopic lipid deposition, caused by an increase in circulating FFAs. The fasting FFA levels in the HFD group were not significantly different from the SD group, and the HFD-GA50 group had significantly lower FFA levels compared to the HFD group (Fig. 4A). In contrast, serum TAG and TC levels were not significantly different between the HFD-fed groups (Fig. 4B and Fig. 4C). I also observed that liver weight and hepatic TC levels did not change among the groups (Fig. 4D and 4F). However, hepatic TAG contents in the HFD-GA50 group tended to be lower than in the HFD group (Fig. 4E). Taken together, our results suggest that GA supplementation is unlikely to induce lipodystrophy.

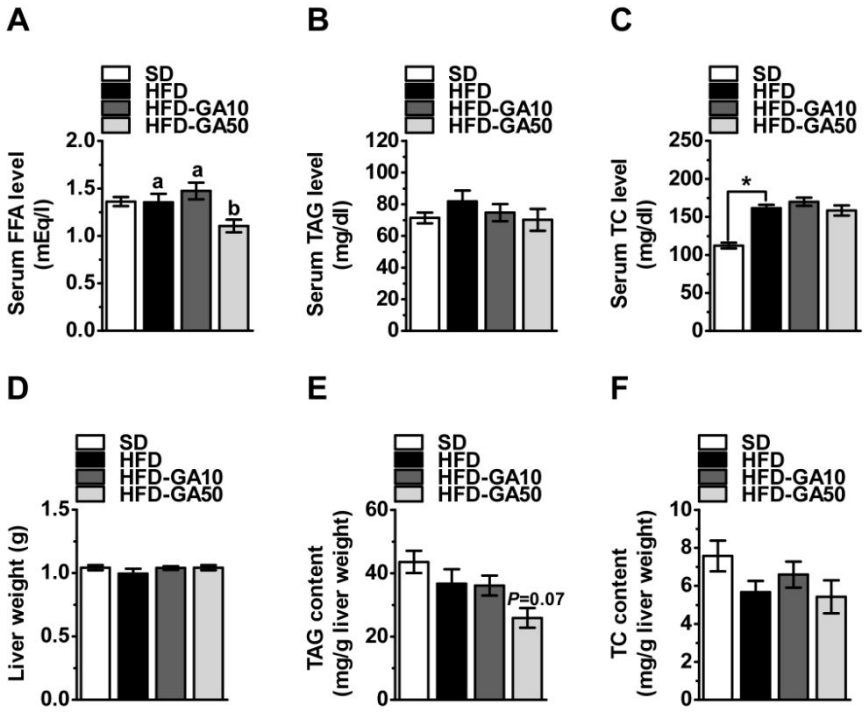

Figure 4. GA treatment reduces serum FFAs and slightly improves hepatic steatosis. Animal experiment was conducted as described at the Materials and Methods section. Lipids in the serum and liver tissue were measured using a commercial kit as described at the Materials and Methods section. (A) Serum FFAs, (B) TAG, and (C) TC concentrations of the experimental groups. (D) Weights of the liver. (E) Hepatic TAG and (F) TC contents. Data are expressed as

means ± SEM. *Significant differences between SD and HFD group. Different letters indicate statistically significant differences between the HFD-treated groups. Differences were considered significant at $P < 0.05$

3.3.4. GA regulates fatty acid metabolism and mitochondrial biogenesis via activation of AMPK in EWAT

Since GA decreased circulating FFA levels, I next analyzed lipolysis-related protein expression in EWAT. I sought to determine whether the expression of ATGL, HSL proteins, and the phosphorylation of HSL at S565 were affected by GA treatment. ATGL expression in HFD-fed mice was 40% lower than in SD-fed mice, whereas the HFD-GA50 group showed significantly higher ATGL expression than the HFD-fed mice (Fig. 5A and Fig. 5B). HFD feeding dramatically increased HSL expression compared with that of the SD group, and this increase was significantly inhibited by GA50 administration (Fig 5A, 5C). In contrast, p-HSL (Ser565) levels tended to be lower in the HFD group than for SD, but this effect was not significant, and the phosphorylated HSL levels in the HFD group were significantly increased by treatment with GA 50 mg/kg (Fig 5A, 5D). These results suggest that GA inhibits lipolysis by inhibiting HSL activity in EWAT. I next investigated whether the expression of SREBP-1 and FAS is regulated by GA treatment to

examine the effect of GA on lipogenesis in EWAT. As shown in Figure 5E-5G, GA significantly reduced the expression of SREBP-1 and FAS.

In these results, I noted an increase in ATGL expression by GA (Fig. 5A and 5B), which was able to mediate TAG hydrolysis, inducing partial lipolysis. Because FFAs released by partial lipolysis can be used as a source of β-oxidation, I next examined the expression of β-oxidation-related genes. GA significantly increased *ppara*, *acsl1*, and *cpt2* gene expression (Fig. 6A-6C), but did not affect *cpt1b* gene expression (data not shown). I also observed that GA significantly enhanced mitochondrial biogenesis-related genes such as *ppargc1a*, *Nrf1*, and *Tfam* in EWAT (Fig. 6D-6F).

To further investigate the mechanisms responsible for how GA regulates fatty acid metabolism and mitochondrial biogenesis, I assessed AMPK activity in EWAT. As expected, p-AMPK and p-ACC expression levels down-regulated by HFD were significantly recovered by treatment with GA 50 mg/kg (Fig. 7A and 7B). These results indicate that GA regulates fatty acid metabolism (such as lipolysis, lipogenesis, and fatty acid oxidation) and mitochondrial

biogenesis by activating AMPK in EWAT.

Lipolysis

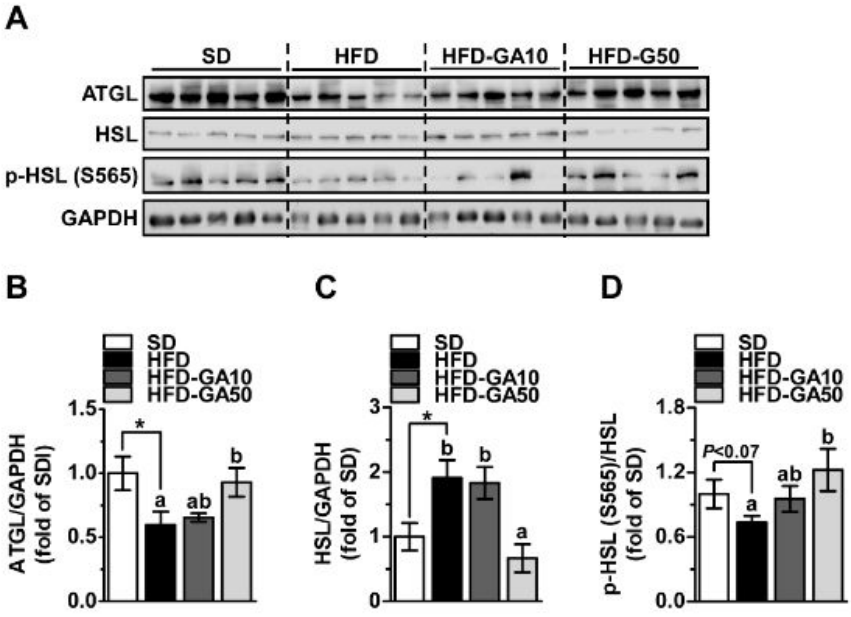

Lipogenesis

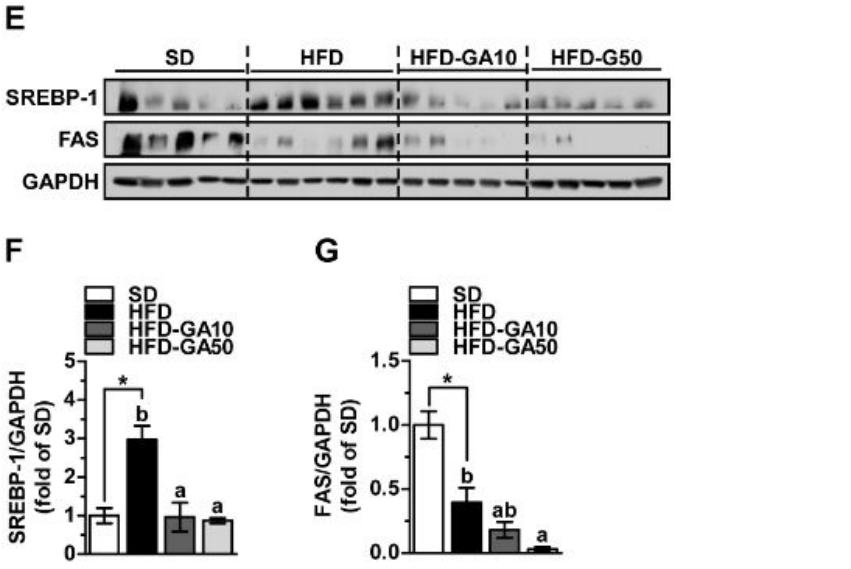

Figure 5. GA treatment regulates the expression of lipolysis and lipogenesis related proteins in EWAT. Mice were fed as described in Figure 1 and EWAT was isolated. A. Western blot analysis of (A) ATGL, HSL, p-HSL (S565) in EWAT of mice fed with SD, HFD, HFD-GA10, or HFD-GA50. GAPDH was used as a loading control. (B-D) The expression levels were quantified using Image J software (National Institutes of Health). Western blot analysis of (E) SREBP-1 and FAS in EWAT of experimental groups. GAPDH was used as a loading control. (F, G) Each bar represents mean ± SEM. Significantly different from the SD-fed group (*$P < 0.05$). Means with different letters are significantly different among the HFD feeding groups ($P < 0.05$)

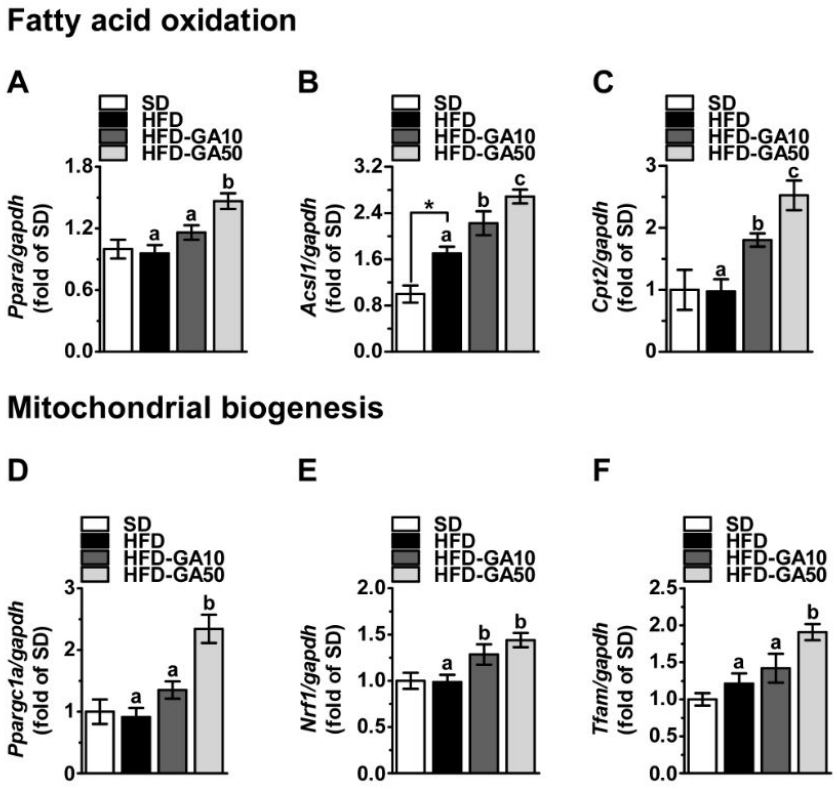

Figure 6. GA treatment increases fatty acid oxidation and mitochondrial biogenesis related gene expression in EWAT. The mice were fed with SD, HFD, and HFD with 10 or 50 mg/kg as described in Figure 1. Total RNA was isolated and qRT-PCR was performed. (A-C) Fatty acid oxidation related genes (*ppara*, *acsl1*, and *cpt2*). (D-F) Mitochondrial biogenesis related genes (*ppargc1a*, *nrf1*, and *tfam*). *Significant differences between SD and HFD

group. Different letters indicate statistically significant differences between the HFD-treated groups. Differences were considered significant at $P < 0.05$

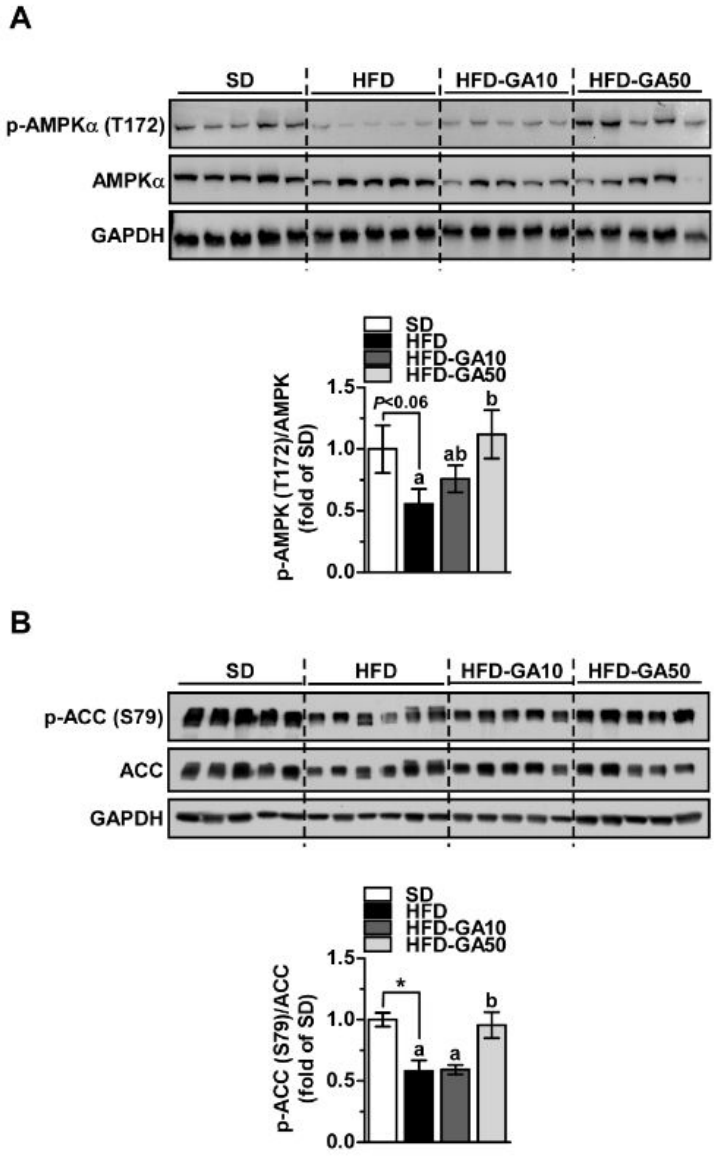

Figure 7. GA treatment increases the phosphorylation of AMPK and ACC in EWAT. (A, B) EWAT were subjected to Western blot analysis using antibodies specific for p-AMPKα (T172), p-ACC

(S79), and total AMPK. GAPDH was used as a loading control. Representative blots are shown in upper layer. Quantitative data represents the mean ± SEM. *Significantly different from the SD-fed group ($P < 0.05$). Means with different letters are significantly different among the HF feeding groups ($P < 0.05$)

3.4. Discussion

GA, an active diarylheptanoid present in ginger, can be considered as the most bioactive compound present in ginger with regards to the attenuation of obesity, as GA elicits potent inhibitory effects on adipogenesis and lipid accumulation in 3T3-L1 cells (Chapter 2). To evaluate that effect of GA *in vivo*, I performed an animal experiment using C57BL/6J mice fed on an HFD. The diet-induced obesity (DIO) mouse model has been widely used for studying obesity and its complications [18]. I observed that GA exerts anti-obesity effects in HFD-fed mice without altering overall diet consumption levels. A post mortem examination showed that the mice fed with HFD-GA50 lost their body weight via a loss of fat mass. Such loss of fat can potentially cause lipodystrophy, leading to ectopic lipid deposition especially in the liver [19]. Thus, I next examined serum and liver lipid concentrations to determine the effect of GA on lipodystrophy. Circulating FFAs and hepatic TAG content were ameliorated to some extent by treatment with GA at 50 mg/kg. Consistently, GA reduced lipogenesis while increasing fatty acid oxidation and mitochondrial biogenesis in EWAT.

Over the past few decades, energy expenditure in adipose tissue has not received widespread attention because its resting metabolic rate is relatively lower than for other metabolic organs such as the liver and muscle [6]. However, recent studies have suggested that the induction of energy expenditure via fatty acid oxidation in WAT is a promising strategy to combat obesity [20-22]. Activating AMPK is a potential strategy to treat obesity and metabolic disorders by inhibiting anabolic pathways and enhancing catabolic pathways. For example, metformin, a drug for type 2 diabetes, has an effect on obesity and diabetes via the activation of AMPK [11]. Thus, I further conducted Western blot analysis to determine whether GA regulates fatty acid metabolism by activation of AMPK. I found that GA activates AMPK in EWAT, and that GA and metformin both increase AMPK activity but in distinct organs, with GA activating AMPK only in adipose tissue (data not shown), with metformin activating it in the liver and muscle. However, further studies are necessary to determine how GA specifically activates AMPK in EWAT.

In conclusion, GA, a polyphenol compound present in

ginger, suppresses body weight gain induced by HFD feeding, which primarily involves a decrease in fat mass via the regulation of fatty acid metabolism and mitochondrial biogenesis by activating AMPK in EWAT. On the basis of these results, I suggest that GA may be used as a potential therapeutic candidate for the treatment of obesity.

3.5. Reference

1. Guyenet, S.J. and M.W. Schwartz, Clinical review: Regulation of food intake, energy balance, and body fat mass: implications for the pathogenesis and treatment of obesity. J Clin Endocrinol Metab, 2012. 97(3): p. 745-55.
2. Scherer, P.E., Adipose tissue: from lipid storage compartment to endocrine organ. Diabetes, 2006. 55(6): p. 1537-45.
3. Ducharme, N.A. and P.E. Bickel, Lipid droplets in lipogenesis and lipolysis. Endocrinology, 2008. 149(3): p. 942-9.
4. Duncan, R.E., et al., Regulation of lipolysis in adipocytes. Annu Rev Nutr, 2007. 27: p. 79-101.
5. Gaidhu, M.P. and R.B. Ceddia, The role of adenosine monophosphate kinase in remodeling white adipose tissue metabolism. Exerc Sport Sci Rev, 2011. 39(2): p. 102-8.
6. Flachs, P., et al., Stimulation of mitochondrial oxidative capacity in white fat independent of UCP1: a key to lean

phenotype. Biochim Biophys Acta, 2013. 1831(5): p. 986-1003.

7. Qi, L., et al., TRB3 links the E3 ubiquitin ligase COP1 to lipid metabolism. Science, 2006. 312(5781): p. 1763-6.
8. Rosen, E.D. and B.M. Spiegelman, Adipocytes as regulators of energy balance and glucose homeostasis. Nature, 2006. 444(7121): p. 847-53.
9. Arner, P., et al., Dynamics of human adipose lipid turnover in health and metabolic disease. Nature, 2011. 478(7367): p. 110-3.
10. Towler, M.C. and D.G. Hardie, AMP-activated protein kinase in metabolic control and insulin signaling. Circ Res, 2007. 100(3): p. 328-41.
11. Lee, Y.S., et al., Berberine, a natural plant product, activates AMP-activated protein kinase with beneficial metabolic effects in diabetic and insulin-resistant states. Diabetes, 2006. 55(8): p. 2256-64.
12. Chen, S., et al., Resveratrol inhibits cell differentiation in 3T3-L1 adipocytes via activation of AMPK. Can J Physiol Pharmacol, 2011. 89(11): p. 793-9.

13. Choi, K.M., et al., Sulforaphane attenuates obesity by inhibiting adipogenesis and activating the AMPK pathway in obese mice. J Nutr Biochem, 2014. 25(2): p. 201-7.
14. Gonzalez-Castejon, M. and A. Rodriguez-Casado, Dietary phytochemicals and their potential effects on obesity: a review. Pharmacol Res, 2011. 64(5): p. 438-55.
15. Sharpe, P.A., et al., Availability of weight-loss supplements: Results of an audit of retail outlets in a southeastern city. J Am Diet Assoc, 2006. 106(12): p. 2045-51.
16. Venkateswarlu, S., et al., Synthesis of gingerenone-A and hirsutenone. Indian Journal of Chemistry Section B-Organic Chemistry Including Medicinal Chemistry, 2001. 40(6): p. 495-497.
17. Min, S.Y., et al., Cocoa polyphenols suppress adipogenesis in vitro and obesity in vivo by targeting insulin receptor. Int J Obes (Lond), 2013. 37(4): p. 584-92.
18. Wang, C.Y. and J.K. Liao, A mouse model of diet-induced obesity and insulin resistance. Methods Mol Biol, 2012. 821: p. 421-33.

19. Huang-Doran, I., et al., Lipodystrophy: metabolic insights from a rare disorder. J Endocrinol, 2010. 207(3): p. 245-55.
20. Jbilo, O., et al., The CB1 receptor antagonist rimonabant reverses the diet-induced obesity phenotype through the regulation of lipolysis and energy balance. FASEB J, 2005. 19(11): p. 1567-9.
21. Boudina, S. and T.E. Graham, Mitochondrial function/ dysfunction in white adipose tissue. Exp Physiol, 2014. 99(9): p. 1168-78.
22. Semple, R.K., et al., Expression of the thermogenic nuclear hormone receptor coactivator PGC-1alpha is reduced in the adipose tissue of morbidly obese subjects. Int J Obes Relat Metab Disord, 2004. 28(1): p. 176-9.

Chapter 4.

Gingerenone A suppresses adipose tissue inflammation and improves glucose intolerance in mice fed with a high-fat diet

Abstract

Chronic low-grade inflammation represents a mechanistic link between obesity and insulin resistance. Several studies have demonstrated that ginger extract exhibits significant anti-inflammatory properties. In this study, I evaluated the effects of Gingerenone A (GA), a major polyphenol compound present in ginger, on inflammation and glucose metabolism in adipose tissue. I observed that GA suppresses adipose tissue inflammation by blocking macrophage recruitment and down-regulating pro-inflammatory cytokines. Consistent with this effect, GA improved glucose intolerance by enhancing whole-body glucose uptake in mice fed on a high-fat diet. These results suggest that GA has therapeutic potential for improving glucose intolerance through the suppression of adipose tissue inflammation.

4.1. Introduction

White adipose tissue (WAT) is composed of an adipose portion and a stromal vascular fraction that includes preadipocytes, mesenchymal stem cells, vascular endothelial cells, and various leucocytes [1]. Resident leucocytes in lean WAT elicit immune responses such as antigen removal to protect the body from infection [2]. In conditions of obesity, however, WAT contains greater numbers of resident leucocytes, especially macrophages. The paracrine interactions between adipocytes and these macrophages further influence obesity-related inflammation. Such chronic low-grade inflammation in obese WAT is then a contributing factor to insulin resistance [3-5].

Adipose tissue macrophages can be categorized as M1 or M2 macrophages according to their distinguishing surface markers

including F4/80, CD11c, and CD206/mannose receptor C type 1 (Mrc1) [6]. M1 macrophages are characterized by $F4/80^{+}$ $CD11c^{+}$ $CD206^{-}$, whereas M2 macrophages typically express $F4/80^{+}$ $CD11c^{-}$ $CD206^{+}$ [6]. M1 or pro-inflammatory macrophages are more dominant than M2 or anti-inflammatory macrophages in conditions of obese obesity, thereby accelerating adipose tissue inflammation [7].

WAT acts not only as an energy storage depot but also as an endocrine organ. WAT releases various adipokines including hormones, cytokines, and chemokines, which are important for maintaining metabolic homeostasis, as well as regulating glucose and lipid metabolism [8]. Numerous studies have reported that several adipokines are abnormally secreted in obese subjects. While adiponectin/adipocyte complement-related protein (ACRP30) is significantly decreased [9], pro-inflammatory cytokines including tumor necrosis factor-α (TNF-α), and chemokines such as monocyte chemoattractant protein (MCP)-1, a member of the CC chemokine superfamily, are increased in the obese state [5]. MCP-1 and/or free fatty acids released from adipocytes attract monocytes/macrophages,

and the recruited macrophages subsequently secrete pro-inflammatory cytokines [2].

I have previously demonstrated that GA, a diarylheptanoid compound present in ginger, elicits anti-adipogenic and anti-lipogenic effects *in vitro* (Chapter 2), as well as anti-obesity effects *in vivo* (Chapter 3). However, the effect of GA on adipose inflammation and glucose metabolism has not been thoroughly investigated.

In this chapter, I sought to examine whether GA elicits anti-inflammatory properties and regulates glucose metabolism resulting in an improvement in insulin resistance in obese mice fed on a high-fat diet (HFD).

4.2. Materials and Methods

4.2.1. Chemicals and reagents

GA was synthesized from curcumin following a method described previously [10]. Antibodies against glyceraldehyde-3-phosphate dehydrogenase (GAPDH) were purchased from Sigma Chemical (St. Louis, MO). Antibodies against adiponectin were obtained from Cell Signaling Biotechnology (Beverly, MA).

4.2.2. Culture of macrophages and 3T3-L1 adipocytes

Murine macrophage RAW 264.7 cells were cultured in Dulbecco's modified Eagle's medium (DMEM) supplemented with 10% fetal bovine serum, 100,000 U/L penicillin, and 100 mg/L streptomycin

at 37℃ and 5% CO_2 atmosphere. 3T3-L1 preadipocytes were cultured in a basal medium consisting of DMEM supplemented with 10% newborn calf serum, and 100,000 U/L penicillin, 100 mg/L streptomycin at 37℃ in a 5% CO_2 atmosphere. Differentiation of the 3T3-L1 preadipocytes was induced by adipogenic agents (0.5 mM 3-isobutyl-1-methylxanthine (IBMX), 1 μM dexamethasone (DEX), and 10 μg/ml insulin) in DMEM containing 10% FBS for 2 days after the cells had reached confluence (Day 0-2). The cell culture medium was then exchanged to a maturation medium, consisting of the basal medium with 10 μg/ml insulin, and cells were incubated for 2 days (Day 2-4). Finally, the medium was changed to DMEM containing 10% FBS (Day 4-6).

4.2.3. Trans-well migration assay

RAW264.7 macrophages were plated onto filters in 6.5 mm trans-well inserts in 24-well plates at 2.5×10^4 cells/filter and treated with GA (10 μM). The lower chamber of the well was filled with DMEM in the presence or absence of 3T3-L1 conditioned medium (CM) and 0.1% bovine serum albumin (BSA). Cells were

then incubated for 2 h. Cells that had migrated into the Type IV collagen-coated membrane were stained with hematoxylin and eosin (H&E) and counted using Image J software (National Institutes of Health).

4.2.4. Co-culture of adipocytes and macrophages

Adipocytes and macrophages were co-cultured in a contact system. RAW 264.7 macrophages (5 x 10^4 cells/ml) were plated with differentiated 3T3-L1 adipocytes, and the co-cultures were incubated in serum-free DMEM for 2 h. As a control, adipocytes and macrophages, the numbers of which were equal to those in the co-culture system, were cultured separately and mixed after harvest. GA was added to the co-cultures at 10 μM.

4.2.5. Quantitative real-time polymerase chain reaction (qRT-PCR)

Total RNA was extracted from cultured cells and epididymal white adipose tissue (EWAT) using an Ambion® RNA isolation kit (Life Technologies, Gaithersburg, MD). cDNA was synthesized with PrimeScript™ 1st strand cDNA Synthesis Kit

(Takara, Kyoto, Japan). qRT-PCR was conducted by using primers and SYBR Green Master Mix (BioRad, Hercules, CA) with a Bio-Rad CFX96 real-time PCR detection system (BioRad, Hercules, CA). The forward and reverse primers for each transcript were as follows: *ccl2*: CCA CTC ACC TGC TGC TAC TCA T and TGG TGA TCC TCT TGT AGC TCT CC; *tnfa*: CCA AGG CGC CAC ATC TCC CT and GCT TTC TGT GCT CAT GGT GT; *itgax*: CTG GAT AGC CTT TCT TCT GCT G and GCA CAC TGT GTC CGA ACT C; *cd68*: AGC TCC CTT GGG CCA AAG and AGG TGA ACA GCT GGA GAA AGA ACT; *mrc1*: CTC GTG GAT CTC CGT GAC AC and GCA AAT GGA GCC GTC TGT GC; *acrp30*: GCT CCT GCT TTG GTC CCT CCA C and GCC CTT CAG CTC CTG TCA TTC C; *gapdh*: CAA GGA GTA AGA AAC CCT GGA CC and CGA GTT GGG ATA GGG CCT CT.

4.2.6. Western blot analysis

EWATs were lysed with RIPA buffer (Cell Signaling Biotechnology) and centrifuged (24,100 x g, 4^{o}C, 10 min) to collect supernatant layers, excluding the layer of fat. The proteins were

loaded onto sodium dodecyl sulfate-polyacrylamide gel electrophoresis (SDS-PAGE) gels and transferred to polyvinylidene fluoride (PVDF) membranes (Millipore, Marlborough, MA). The membranes were blocked with 5% skim milk and incubated with specific primary antibodies followed by horseradish peroxidase (HRP)-conjugated secondary antibodies. Protein bands were visualized using a chemiluminescence detection kit (Amersham Pharmacia Biotech; Piscataway, NJ).

4.2.7. Histological analysis

EWATs were fixed in 4% formaldehyde and embedded in paraffin. To determine the effect of dietary GA on macrophage infiltration in EWATs, 3-μm-thick sections were processed as described [11], using mouse monoclonal anti-CD68 antibodies at dilutions of 1/200 (Abcam, Cambridge, MA). The sections were then immunostained with HRP polymer (Ultravision^{TM} LP Large Volume Detection System; Thermo Fisher Scientific, Fremont, CA) in accordance with the manufacturer's specifications. Crown-like structures and CD68-positive cells were counted using Image J software (National Institute of Health, Bethesda, MD).

4.2.8. Experimental animals and diets

(A) *Effect of GA on adipose tissue inflammation in mice*

All experiments were approved by the Seoul National University Animal Experiments Ethics Committee. Six-week-old male C57BL/6 mice were purchased from Japan SLC Inc. (Hamamatsu, Shizuoka, Japan) and acclimated for 1 week, with free access to chow and water. A total of 47 mice were randomly distributed into the following four groups; a standard diet (SD, D12450B Rodent Diet with 10 kcal% fat; Research Diets, Inc., NJ, USA) (12 mice), a high-fat diet (HFD, D12492 Rodent Diet with 60 kcal% fat; Research Diets) (12 mice), HFD plus 50 mg/kg body weight GA (HFD-GA50; 12 mice), or HFD plus 10 mg/kg body weight GA (HFD-GA10; 11 mice). The diets were purchased from Research Diets, Inc. (New Brunswick, NJ) and provided in the form of pellets for 15 weeks. GA was dissolved in polyethylene glycol (PEG) 200 and introduced to the animals by oral gavage every day. After 15 weeks of treatment, mice were sacrificed under intraperitoneal Zoletil/Rompun anesthesia after an overnight fast,

and all efforts were made to minimize suffering. Blood samples were collected from the heart chambers. After collecting blood, several tissue samples were promptly removed, rinsed with PBS and weighed. EWATs were snap-frozen in liquid nitrogen and stored at -80℃ for RNA and protein analysis.

(B) *Effect of GA on insulin resistance in mice*

The animal studies were conducted in accordance with the guidelines of the Institutional Animal Care and Use Committee of the University of Massachusetts Medical School. Inbred twenty 2- to 3-month-old male C57BL/6 mice were randomly divided into three groups: chow diet (CD, LabDiet 5001; ~4.5% kcal from fat; LabDiet, St Louis, Missouri, USA)-fed, HFD (Harlan Teklad TD 93075; 55% kcal from fat; Harlan Laboratories, Indianapolis, IN, USA)-fed, and HFD plus GA at 100 mg/kg (HFD-GA100)-fed.

4.2.9. Intraperitoneal glucose tolerance test

After the mice were fed a chow or an HFD diet with or without GA for 14 weeks, they were subjected to an intraperitoneal glucose tolerance test (IPGTT). IPGTT was performed after an

overnight fast. Blood samples were taken at 0, 15, 30, 60, 90, and 120 min after intraperitoneal injection of glucose (1g/kg body weight) as previously described [12].

4.2.10. Hyperinsulinemic-euglycemic clamp to assess insulin action *in vivo*

The mice fed a CD or an HFD diet with or without GA for 15 weeks were fasted overnight (~15 h), and a 2 h hyperinsulinemic-euglycemic clamp was applied in conscious mice with a primed and continuous infusion of human insulin (150 mU/kg body weight priming followed by 2.5 mU/kg/min; Humulin®, Eli Lilly and Company, Indianapolis, IN), and 20% glucose was infused at variable rates to maintain euglycemia, as described previously [12]. [3-^{3}H]glucose (PerkinElmer, Waltham, MA, USA) was continuously infused to assess whole-body glucose turnover, and 2-deoxy-D-[1-^{14}C]glucose (2-[^{14}C]DG; PerkinElmer Life and Analytical Sciences) was administered as a bolus (10 μCi) at 75 min after the start of clamping to estimate insulin-stimulated glucose uptake in individual tissues as previously described [12].

Blood samples were taken before, during, and at the end of clamping for measurement of plasma [3-^{3}H]glucose, $^{3}H_2O$, 2-[^{14}C]DG, and insulin concentrations. At the end of the clamping, mice were sacrificed under intraperitoneal Zoletil/Rompun anesthesia, and all efforts were made to minimize suffering.

4.2.11. Biochemical analysis and calculation

Glucose concentration during clamping was analyzed using a glucose oxidase method with a GM9 Analyzer (Analox Instruments, Ltd., Hammersmith, London, UK). Plasma insulin concentration was measured with ELISA kits (ALPCO Diagnostics, Salem, NH, USA). Plasma concentrations of [3-^{3}H]glucose, 2-[^{14}C]DG, and $^{3}H_2O$ were determined after deproteinization of the plasma samples, as previously described [12]. For the determination of tissue 2-[^{14}C]DG-6-P content, tissue samples were homogenized, and the supernatants were subjected to an ion exchange column to separate 2-DG-6-P from 2-DG. Hepatic glucose production during the clamping was determined by subtracting the glucose infusion rate from the whole-body glucose uptake rate. Glucose uptake in

individual tissues was calculated from the plasma 2-[^{14}C]DG clearance profile [12].

4.2.12. Statistical analysis

Data are expressed as means ± standard error of mean (SEM). Student's *t*-test was used for single statistical comparisons. One-way ANOVA with *post hoc* Duncan's test were used to determine whether GA had a significant effect on HFD-fed mice. A probability value of $P < 0.05$ was used as the criterion for statistical significance.

4.3. Results

4.3.1. GA suppresses macrophage recruitment and modulates pro-inflammatory adipokine expression *in vitro*

Chronic low-grade inflammation induced by obesity is strongly associated with insulin resistance. Recent studies have identified macrophage infiltration in adipose tissue, suggesting an important link with inflammatory responses. I first examined the effect of GA at 10 μM (a non-cytotoxic concentration), on

macrophage infiltration into adipocyte-conditioned medium using a trans-well system. As shown in Figures 1A and 1B, the adipocyte-conditioned medium resulted in significantly induced Raw264.7 macrophage migration, and GA treatment strongly inhibited this migration. This indicates that treatment with GA has an inhibitory effect on adipocyte-CM-induced macrophage chemotaxis.

To further investigate the mechanisms underlying the GA-inhibited macrophage migration observed, I examined the changes in expression of chemokine *ccl2* and pro-inflammatory marker *tnfa* using a co-culture contact system. Co-cultures of differentiated 3T3-L1 adipocytes and Raw264.7 macrophages in the contact system up-regulated the expression of *ccl2* and *tnfa* in comparison to the control group ($P < 0.05$). GA significantly decreased *tnfa* by ~61% and decreased *ccl2* by ~45% although without statistical significance (Fig. 1C and 1D).

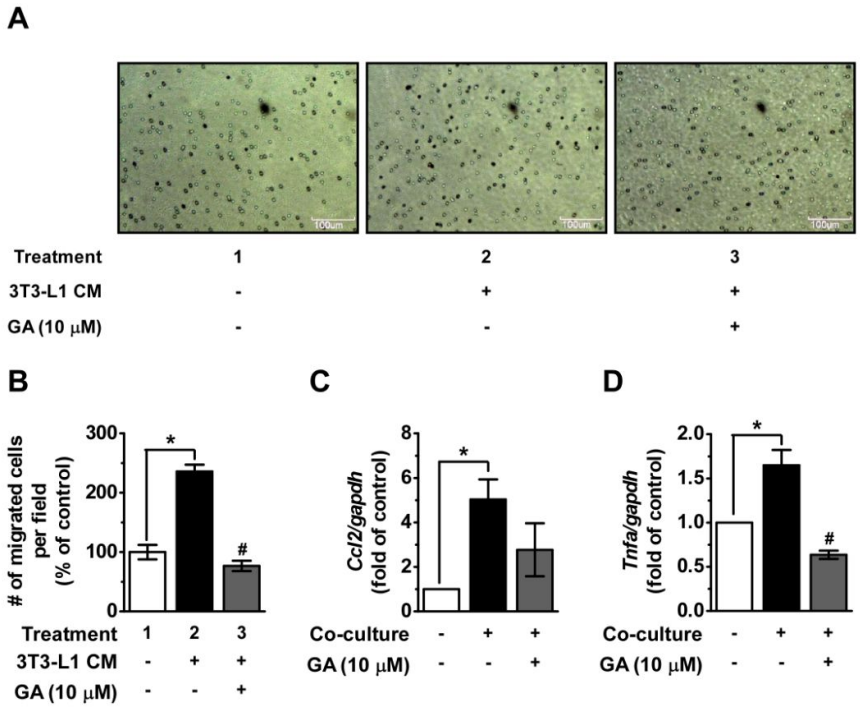

Figure 1. GA inhibits macrophage recruitment and modulates

adipokines expression. (A) The migration of RAW264.7 cells through a type IV collagen-coated transwell filter was assessed with 3T3-L1 CM and GA (10 μM). Cells were incubated for 2 h. Photographs of migrated H&E stained cells are shown (× 100). (B) Quantitative analysis of the migrated cells. (C-D) Alteration of gene expression of pro-inflammatory adipokines by co-culture in the contact system. RAW264.7 cells were plated in 6-well plate containing differentiated 3T3-L1 cells. As a control, RAW264.7 cells and differentiated 3T3-L1 cells were separately cultured. After 2 h incubation, total RNA was isolated from RAW264.7 cells and 3T3-L1 cells (control) and RAW264.7/3T3-L1 co-cultures (co-culture), and real-time RT-PCR was performed. Each bar represents the mean ± SEM (n = 3). Values were analyzed using unpaired Student's *t*-test. $^{*}P < 0.05$ control *vs.* co-culture control, $^{\#}P < 0.05$ GA-treated *vs*. co-culture control.

4.3.2. GA administration inhibits HFD-induced macrophage infiltration into adipose tissue

I next examined the effect of GA on adipose tissue inflammation *in vivo*. Histological examination revealed that the number of crown-like structures in EWAT samples in the HFD group were higher than those in the SD group, which were reduced after GA supplementation (Fig. 2A and 2B). Moreover, consistent with the *in vitro* results (Fig. 1A and 1B), GA suppressed HFD-induced increases in the expression of the CD68 gene and protein in a dose-dependent manner (Fig. 2C and 2D).

It is generally accepted that monocytes expressing the M1 marker are significantly higher, while monocytes expressing the M2

marker are lower overall in obese adipose tissue samples compared with non-obese adipose tissue [7]. I examined the expression of *itgax*, an M1 macrophage marker in adipose tissue. HFD significantly increased the expression of *itgax* in adipose tissue, implying the presence of inflammatory macrophages. GA also reduced *itgax* expression significantly in the obese EWAT samples (Fig. 2E). I then analyzed the expression of *mrc1,* an M2 macrophage marker in adipose tissue. Unlike *itgax,* expression of *mrc1* was not changed significantly by HFD feeding. However, GA did significantly increase *mrc1* expression in the obese EWAT samples (Fig. 2F). Taken together, these results indicate that GA suppresses monocyte/macrophage infiltration and improves the balance between M1 and M2 macrophages characterized by expression of *itgax* and *mrc1,* respectively, in obese EWAT samples.

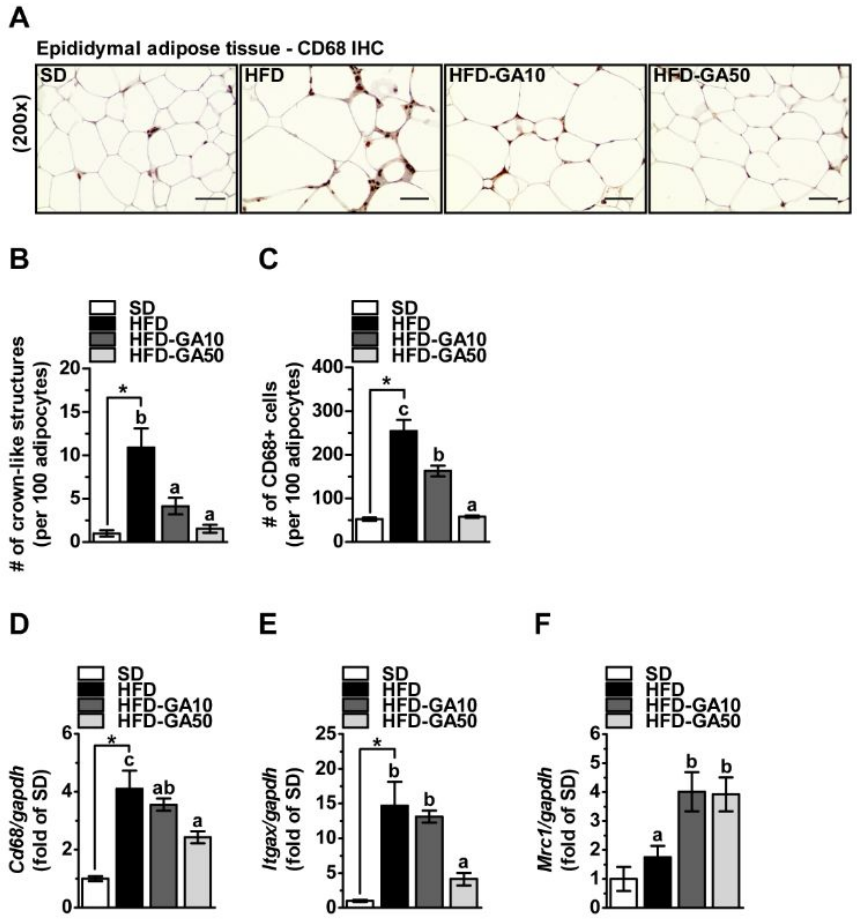

Figure 2. GA prevents aggravation of macrophage infiltration induced by HFD in EWAT. Six-week-old male C57BL/6 mice were fed a SD, an HFD, or HFD plus 10 mg/kg (HFD-GA10), or HFD plus 50 mg/kg (HFD-GA50) for 15 weeks. (A) Immunohistochemical (IHC) detection of CD68 in EWAT.

Macrophages are stained brown. (200x), (B) number of crown-like structures, and (C) total number of infiltrated monocyte/macrophage into EWAT. It was quantified by counting CD68-positive cells per 100 adipocytes. (D) *Cd68*, (E) *itgax*, (F) *mrc1* expression in EWAT. All values were normalized to *gapdh*; * Significant difference from the SD feeding group ($P < 0.05$). Means with different letter are significantly different among HFD feeding groups ($P < 0.05$).

4.3.3. GA reduces adipose tissue inflammation by regulating adipokines

Next, I investigated the expression of cytokines, which are responsible for regulating the recruitment of macrophages and inflammation in adipose tissue. GA downregulated expression of *ccl2* (a macrophage attractant), which was upregulated by HFD at a concentration of 50 mg/kg in the EWAT samples (Fig. 3A). In addition, GA suppressed the expression of the proinflammatory cytokine, *tnfa*, which was also upregulated by HFD in a dose-dependent manner in EWAT (Fig. 3B).

I then analyzed the expression of genes and proteins in EWAT samples and bloodstream levels of adiponectin, an adipokine with anti-inflammatory, insulin-sensitizing effects in obese mice. At a concentration of 50 mg/kg, GA increased both adiponectin gene and protein expression in the obese EWAT samples (Fig. 3C and 3D). However, the increment in adiponectin levels in EWAT was not concomitant with a rise in adiponectin levels in the bloodstream (Fig. 3E). These results suggest that GA may be preventing local inflammation in EWAT by downregulating inflammatory cytokines

and upregulating anti-inflammatory cytokines.

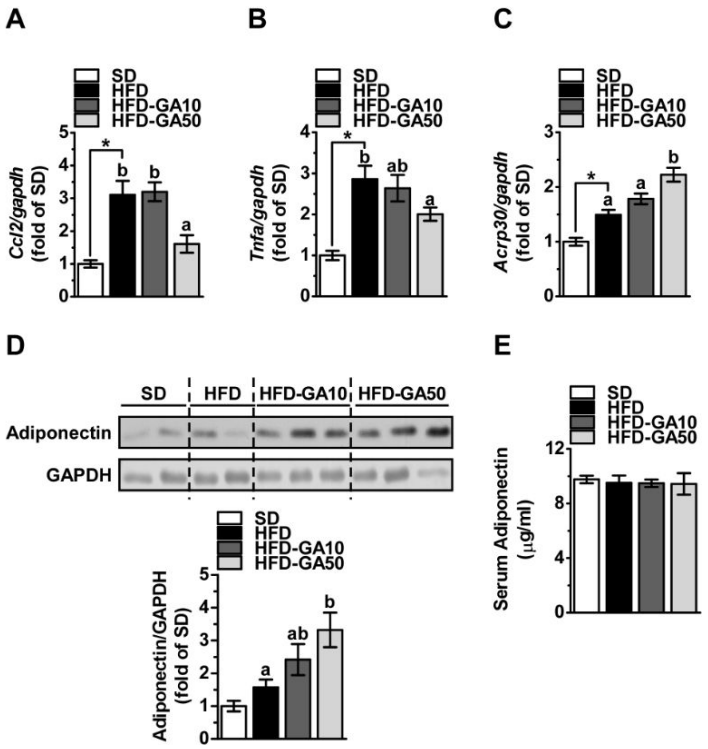

Figure 3. Effects of GA on inflammation-related cytokines obese EWAT. (A) *Ccl2* expression, (B) *tnfa* expression, and (C) *acrp30* expression in EWAT. (D) Adiponectin protein expression in EWAT. GAPDH was used as internal control to normalize the values (E) Serum adiponectin concentrations; Significant differences between the group treated with SD and HFD (*$P < 0.05$). Means with different letter are significantly different from each other among HFD feeding groups ($P < 0.05$).

4.3.4. GA improves glucose intolerance induced by HFD

To investigate the effect of GA on glucose metabolism, I performed a GTT. Blood glucose levels in the fasted condition were initially not significantly different in any groups. However, blood glucose levels in the HFD-GA100 group were lower than the HFD group as determined by the GTT, especially at 15 min and 60 min (Fig. 4A). In addition, GA improved HFD-induced glucose intolerance characterized as evident by its AUC value (Fig. 4B). To elucidate whether the effect of GA on glucose metabolism correlated with circulating adiponectin concentrations, I conducted an ELISA analysis using the plasma samples. Administration of GA at a concentration of 100 mg/kg significantly increased circulating adiponectin levels in contrast to the group supplemented with GA 10 or 50 mg/kg treatment in the mice fed with HFD (Fig. 4C).

To further determine the effect of GA on glucose homeostasis, I performed a 2-h hyperinsulinemic-euglycemic clamp to measure insulin sensitivity in conscious mice fed on HFD for 15 weeks. Basal (overnight-fasted) plasma insulin and glucose levels were not significantly different between the three groups. Although

plasma glucose levels were maintained at euglycemia during the clamp, the plasma insulin levels were 40% lower in the GA-treated group than in the HF-fed group (2.1 ± 0.5 for HFD vs. 1.3 ± 0.1 for GA-treated group; $P < 0.19$), although this was not significant at the termination of the clamp experiments (Fig. 5A and 5B).

Insulin resistance was induced by HFD feeding, characterized by a decrease in glucose infusion rates by ~57% during the clamp experiments in comparison to the CD group (Fig. 5C). Although a significant difference was not observed in the glucose infusion rate between the HFD and HFD-GA100 ($P < 0.14$) groups, the mean values were approximately 36% higher in the HFD-GA100 group than in the HFD group (15.0 ± 3.6 mg/kg/min for HFD vs. 20.4 ± 0.8 mg/kg/min for HFD-GA100 group) (Fig. 5C). Whole-body glucose turnover was also decreased by HFD feeding by approximately ~28% during the clamp experiments in comparison to the CD group (Fig. 5D). Interestingly, insulin-stimulated whole-body glucose turnover during the clamp experiments was significantly increased in the HFD-GA100 group (32.4 ± 2.0 mg/kg/min) compared to the HFD group (22.7 ± 1.0 mg/kg/min)

(Fig. 5D). In addition, insulin-stimulated whole-body glycolysis showed a similar pattern of changes in terms of whole-body glucose turnover (12.3 ± 1.4 mg/kg/min for HFD vs. 18.6 ± 1.7 mg/kg/min for HFD-GA100 group) (Fig. 5E). Furthermore, basal hepatic glucose production rates did not differ between the HFD-GA100 and HFD groups, and the hepatic insulin action to suppress hepatic glucose production was attenuated in both the HFD-GA100 and HFD groups (Fig. 5F-5H). These results demonstrate that HFD-induced insulin resistance is improved by GA administration, and that these changes are not due to alterations in hepatic glucose metabolism but more likely the result of an alteration occurring in peripheral tissues of the body.

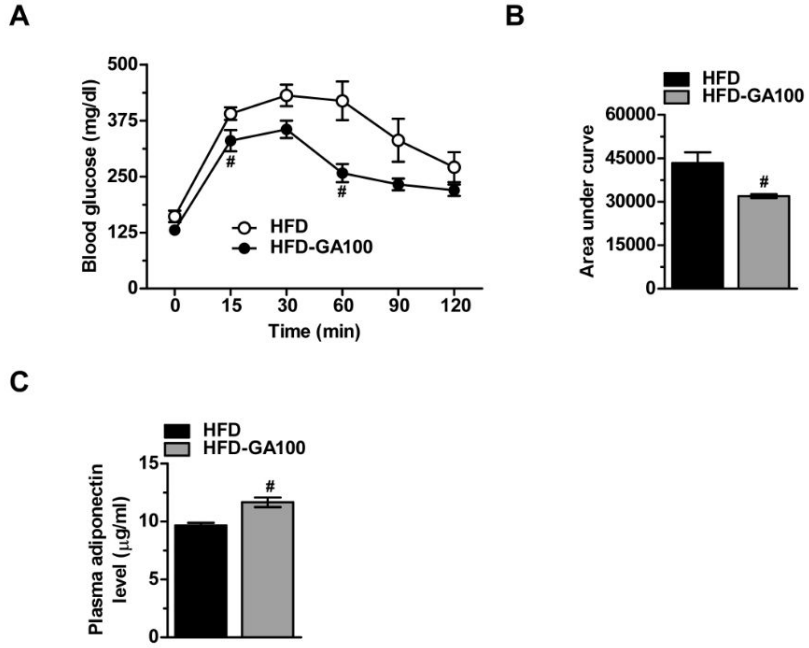

Figure 4. GA administration improves HFD-induced glucose intolerance in mice. Mice at 2- to 3-month-old were fed a HFD (6 mice), HFD plus 100 mg/kg GA (HFD-GA100; 4 mice) for 14 wk. (A) Plasma glucose concentration curves during IPGTT for a high-fat diet with or without GA. (B) The area under the curve (AUC) was significantly different for GA-treated mice versus HFD mice. (C) Plasma adiponectin concentrations. Values are presented as means ± SEM. Values were analyzed by unpaired Student's *t*-test. $^{\#}P < 0.05$ GA-treated vs. HFD mice.

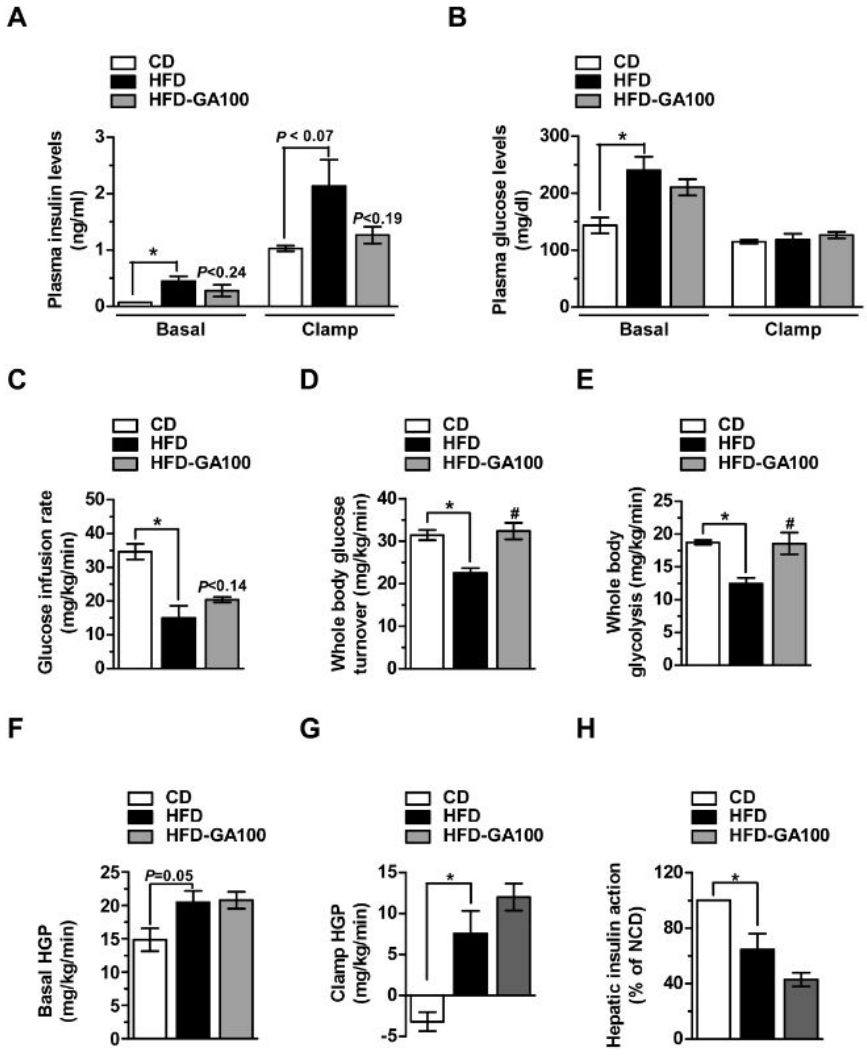

Figure 5. GA improves HFD-induced insulin resistance in mice. Mice at 2- to 3-month-old were fed a HFD (6 mice), HFD plus 100 mg/kg GA (HFD-GA100; 4 mice) for 14, or CD (5 mice) for 15 wk.

(A) Plasma insulin levels were measured with ELISA. Samples were taken from the mice at the beginning and end of hyperinsulinemic-euglycemic clamp experiments. (B) Plasma glucose levels were analyzed by a glucose oxidase method on a GM9 Analyzer. (C) Steady-state glucose infusion rate during the clamp experiments in awake mice. (D) Insulin-stimulated whole-body glucose turnover was calculated by infusion of [^{3}H]glucose during the tests. (E) Insulin-stimulated whole-body glycolysis. (F-H) Basal and clamp hepatic glucose production rates, and hepatic insulin action. Values are presented as means ± SEM. Values were analyzed by unpaired Student's *t*-test. *$P < 0.05$ HFD vs. CD mice. $^{\#}P < 0.05$ GA-treated vs. HFD mice.

4.4. Discussion

Increases in adipocyte lipolysis produce elevated levels of circulating FFAs in the bloodstream, providing a mechanistic link between obesity, inflammation and insulin resistance [13]. Nguyen *et al*. reported that macrophages infiltrate into hypertrophic adipose tissue and secrete inflammation-related cytokines, an activity induced by FFAs [14]. Therefore, substances that exert anti-hypertrophic and anti-lipolytic effects may potentially be useful as anti-inflammatory and insulin-sensitizing agents [15]. I observed that GA suppresses adipocyte hypertrophy and lipolysis in mice fed on HFD (Chapter 3; Fig. 3 and Fig. 5), suggesting the possibility that GA may be used to alleviate inflammation and insulin resistance caused by adipose tissue dysfunction. To elucidate the effects of GA, I first performed a trans-well migration assay with a co-culture contact system. As expected, GA dramatically inhibited macrophage infiltration and significantly reduced the expression of the pro-inflammatory cytokine *tnfa* (Fig. 1 and Fig. 3). TNF-α is known to be overexpressed in adipose tissue in obese humans as well as in animal models, and obese mice show improvements in

insulin sensitivity when TNF-α activity is blocked [16]. Arner *et al.* suggested TNF-α acts at local sites (such as adipose tissue) rather than acting systemically through an autocrine and paracrine mechanism. TNF-α induces the expression of pro-inflammatory cytokines including MCP-1 and IL-6, and suppresses the expression of anti-inflammatory adipokines (such as adiponectin) via inhibition of its promoter activity [17, 18]. MCP-1 plays a major role in the recruitment of monocytes and macrophages to the adipose tissue [1], and I demonstrated that such an inhibitory effect of GA on the MCP-1 gene, *ccl2* expression leads to the suppression of macrophage infiltration into EWAT (Fig. 2 and Fig. 3). A previous study has shown that macrophages surround the dead and dying adipocytes to form a crown-like structure in obese adipose tissue [19]. The number of crown-like structures is indicative of not only the number of dead adipocytes, but also the extent of macrophage recruitment. I observed that GA suppressed the formation of these crown-like structures, suggesting the possibility that GA exerts a protective effect against adipose tissue inflammation (Fig. 2). The administration of GA50 mg/kg did not improve serum glucose or

insulin levels (data not shown) despite GA effectively alleviating adipose tissue inflammation in mice fed on a high-fat diet.

I therefore decided to perform another in-vivo experiment to examine the effect of GA on high-fat diet-induced insulin resistance, and elected to use a higher GA concentration (100 mg/kg). It has been well-documented that insufficient levels of adiponectin/ACRP30 induces insulin resistance in various animal models [9, 20, 21]. I observed that HFD-GA50 significantly increased the expression of adiponectin at both the transcription (*acrp30*) and protein level (Fig. 3). However, the alteration of adiponectin expression in adipose tissue did not correlate with the circulating adiponectin concentrations in all of the groups. Although supplementation of GA 10 or 50 mg/kg did not affect circulating adiponectin levels, administration of GA 100 mg/kg significantly increased plasma adiponectin concentrations compared with the HFD-fed mice (Fig. 3 and Fig. 4). Consistent with this data, oral gavage of GA 100 mg/kg effectively improved glucose intolerance caused by the high-fat diet by increasing whole-body glucose uptake (Fig. 4 and Fig. 5).

An overall reflection on the results obtained in our studies suggests that GA has at least some therapeutic potential for the improvement of glucose intolerance, and it achieves this effect by suppressing adipose tissue inflammation.

4.5. Reference

1. Yu, R., et al., Mesenteric adipose tissue-derived monocyte chemoattractant protein-1 plays a crucial role in adipose tissue macrophage migration and activation in obese mice. Obesity (Silver Spring), 2006. 14(8): p. 1353-62.
2. Kammoun, H.L., M.J. Kraakman, and M.A. Febbraio, Adipose tissue inflammation in glucose metabolism. Rev Endocr Metab Disord, 2014. 15(1): p. 31-44.
3. Xu, H., et al., Chronic inflammation in fat plays a crucial role in the development of obesity-related insulin resistance. J Clin Invest, 2003. 112(12): p. 1821-30.
4. Kern, P.A., et al., Adipose tissue tumor necrosis factor and interleukin-6 expression in human obesity and insulin resistance. Am J Physiol Endocrinol Metab, 2001. 280(5): p. E745-51.
5. Makki, K., P. Froguel, and I. Wolowczuk, Adipose tissue in obesity-related inflammation and insulin resistance: cells,

cytokines, and chemokines. ISRN Inflamm, 2013. 2013: p. 139239.

6. Osborn, O. and J.M. Olefsky, The cellular and signaling networks linking the immune system and metabolism in disease. Nat Med, 2012. 18(3): p. 363-74.
7. Suganami, T. and Y. Ogawa, Adipose tissue macrophages: their role in adipose tissue remodeling. Journal of leukocyte biology, 2010. 88(1): p. 33-39.
8. Galic, S., J.S. Oakhill, and G.R. Steinberg, Adipose tissue as an endocrine organ. Mol Cell Endocrinol, 2010. 316(2): p. 129-39.
9. Maeda, N., et al., Diet-induced insulin resistance in mice lacking adiponectin/ACRP30. Nat Med, 2002. 8(7): p. 731-7.
10. Venkateswarlu, S., et al., Synthesis of gingerenone-A and hirsutenone. Indian Journal of Chemistry Section B-Organic Chemistry Including Medicinal Chemistry, 2001. 40(6): p. 495-497.
11. Byun, S., et al., Luteolin inhibits protein kinase C(epsilon) and c-Src activities and UVB-induced skin cancer. Cancer Res, 2010. 70(6): p. 2415-23.

12. Kim, H.J., et al., Differential effects of interleukin-6 and -10 on skeletal muscle and liver insulin action in vivo. Diabetes, 2004. 53(4): p. 1060-7.
13. Boden, G., Obesity and free fatty acids. Endocrinol Metab Clin North Am, 2008. 37(3): p. 635-46, viii-ix.
14. Nguyen, M.T., et al., A subpopulation of macrophages infiltrates hypertrophic adipose tissue and is activated by free fatty acids via Toll-like receptors 2 and 4 and JNK-dependent pathways. J Biol Chem, 2007. 282(48): p. 35279-92.
15. Nayagam, V.M., et al., SIRT1 modulating compounds from high-throughput screening as anti-inflammatory and insulin-sensitizing agents. J Biomol Screen, 2006. 11(8): p. 959-67.
16. Hotamisligil, G.S., Inflammatory pathways and insulin action. Int J Obes Relat Metab Disord, 2003. 27 Suppl 3: p. S53-5.
17. Arner, P., The adipocyte in insulin resistance: key molecules and the impact of the thiazolidinediones. Trends Endocrinol Metab, 2003. 14(3): p. 137-45.
18. Ruan, H., et al., Profiling gene transcription in vivo reveals adipose tissue as an immediate target of tumor necrosis factor-

alpha: implications for insulin resistance. Diabetes, 2002. 51(11): p. 3176-88.

19. Murano, I., et al., Dead adipocytes, detected as crown-like structures, are prevalent in visceral fat depots of genetically obese mice. Journal of lipid research, 2008. 49(7): p. 1562-1568.
20. Yamauchi, T., et al., The fat-derived hormone adiponectin reverses insulin resistance associated with both lipoatrophy and obesity. Nat Med, 2001. 7(8): p. 941-6.
21. Kubota, N., et al., Disruption of adiponectin causes insulin resistance and neointimal formation. J Biol Chem, 2002. 277(29): p. 25863-6.

국문초록

세계보건기구에 따르면, 과체중과 비만은 에너지 섭취와 소비의 불균형으로 인하여 건강을 위협할 정도로 체내에 과도하게 지방이 축적된 상태로 정의된다. 여러 연구를 통해 비만에 따른 지방조직의 과도한 증가가 제2형 당뇨, 심혈관 질환 또는 비알코올성 지방간 질환과 같은 대사성 질환의 위험 인자로 제시됨으로써, 지방조직의 증가를 억제하는 것이 비만을 예방하거나 치료하기 위한 주요 전략으로 활용되고 있다.

생강은 체중조절용 일반의약품에 가장 빈번하게 사용되는 성분으로 몇몇 연구를 통하여 생강의 비만과 대사성질환 개선 효능이 보고되어 왔지만, 정확히 생강의 어떤 성분이 어떤 기작을 통하여 비만과 대사성 질환에 효능을 보이는 지는 보고되

지 않았다. 따라서, 본 연구에서는 3T3-L1 지방세포주 모델을 활용하여 생강의 주된 활성 성분인 6-진저롤, 8-진저롤, 10-진저롤과 6-쇼가올, 진저레논 에이가 지방세포분화에 미치는 영향을 비교 분석하였다. 그 결과, 생강의 주요 활성 성분들 중에서 진저레논 에이가 3T3-L1 지방전구세포의 분화를 가장 효과적으로 저해함을 확인하였고, 지방세포분화 및 지방합성 조절 단백질의 발현을 농도-의존적으로 저해함을 확인하였다. 또한 생강의 주요 활성 성분들 중에서 진저레논 에이만이 유의적으로 성숙한 지방세포의 지질축적을 저해함을 확인하였다. 이러한 결과들을 통하여 진저레논 에이의 지방조직 증가 저해에 관한 잠재적 능력을 확인할 수 있었다.

이를 바탕으로 고지방식이 섭취로 유도되는 비만 설치류 모델에서 진저레논 에이가 체중조절에 미치는 영향을 연구한 결과, 식이섭취량의 변화 없이 고지방식이 섭취로 유도되는 체중의

증가를 유의적으로 저해함을 확인하였다. 이러한 체중 조절 효능은 비만의 대표적인 특징인 지방조직의 증가를 현저하게 감소시킴으로써 나타남을 확인하였다. 하지만 지방조직이 급격히 부서질 경우, 체내로 유입된 지질이나 지방조직에서 유리된 지방산이 혈류를 통하여 간이나 근육과 같은 대사조절 조직들에 이소성 지질 축적을 유도할 수 있다. 따라서 진저레논 에이가 이러한 지방이상증에 미치는 영향을 확인하기 위하여 혈중 유리지방산과 간 조직 내 지질함량을 확인한 결과, 진저레논 에이 처리는 혈중 유리지방산의 농도와 간조직 내 중성지질의 함량을 낮추었다. 이를 통하여 진저레논 에이는 지방이상증을 초래하지 않고 효과적으로 지방조직의 크기를 감소시킴을 확인할 수 있었다. 그렇다면 어떻게 진저레논 에이가 지방조직의 크기를 저해하는지를 밝히고자 지방산 대사관련 마커들을 확인한 결과, 진저레논 에이 처리에 의하여 지질분해와 지방산 합성관련 단백질의 발현이 저해

되고 유리지방산의 산화와 미토콘드리아 생성관련 전사체의 발현이 증가됨을 확인하였다. 이러한 지방산 대사의 주요 조절인자인 AMP-activated protein kinase (AMPK) 의 인산화가 진저레논에이 처리에 의하여 유의적으로 증가됨으로 보아 진저레논 에이가 지방조직에서 AMPK 를 활성화시켜 지방산 대사를 조절함으로써 체중조절 효능을 보인다는 결론에 도달할 수 있었다.

지방조직의 과도한 증가로 초래되는 지방조직 염증은 인슐린 저항성과 밀접한 관계를 보인다. 따라서 진저레논 에이의 지방조직 저감화에 의한 항비만 효과가 지방조직 염증과 인슐린 저항성에 미치는 영향을 추가적으로 연구하였다. 실험 결과, 진저레논 에이는 대식세포의 유입을 막고 전염증성 싸이토카인인 tumor necrosis factor (TNF-α) 의 발현을 저해함을 확인하였다. 또한 진저레논 에이 처리는 지방조직에서 인슐린 저항성 개선에 도움을 주는 아디포카인인 adiponectin 의 전사체 및 단백체 발

현을 증가시킨다는 것을 확인하였다. 이러한 지방조직의 염증 저해와 adiponectin 증진 효능은 포도당 대사에 영향을 미칠 수 있으므로 고인슐린혈증-정상혈당 클램프 연구를 통해 진저레논 에이가 인슐린 저항성에 미치는 영향을 규명하였다. 그 결과, 진저레논 에이는 몸 전체의 포도당 대사능을 촉진시켜 고지방식이 섭취로 유도된 내당능을 개선시킴을 확인할 수 있었다.

이 결과들을 종합하여 보았을 때, 진저레논 에이는 고지방식이 섭취 동물 모델에서 체중 증가와 지방조직 염증을 저해하며 내당능을 개선시킨다. 따라서, 진저레논 에이는 비만 및 대사성 질환 치료제로써의 개발 가능성이 있을 것으로 사료된다.

검색어 : 진저레논 에이, 비만, 지방조직 염증, 내당능, 지방산 대사

학번 : 2011-30346